UNIVERSITY OF OXFORD

Opinion formation models on networks based on game theory

MMath CCD

CANDIDATE NUMBER
303269

Hilary 2016

Abstract

Sociophysics is a field that studies social behaviour using theories and techniques from topics such as statistical physics. In particular, it has become fashionable to use Monte Carlo simulations to explain and predict sociological phenomena. The Deffuant model is a popular mathematical model in sociophysics. Each individual holds an opinion in a certain real interval, and the opinion distribution of the population evolves with sequential random pairwise encounters. A pair of interacting individuals update their opinions towards a compromise if and only if their opinions differ by less than a given threshold called 'confidence bound'. Incorporating network structure allows one to take into account heterogeneity of interactions in a population. We study the Deffuant model on networks by considering different network structures and interaction mechanisms between pairs of individuals. In particular, we show how convergence time and the number of opinion groups at equilibrium are affected by network topology, confidence bound, the number of participating agents, and their willingness to change their minds. We use numerical simulations to explore the opinion dynamics of the Deffuant model on networks and conduct regression analysis to model observed phenomena.

Acknowledgements

Contents

1 Introduction

Social interactions play a central role in the process of opinion formation in communities [35]. Discussions among acquaintances, coworkers, friends, and family members often lead interlocutors to adjust their viewpoints on politics, participation in social movement, and adoption of technological innovations [63]. Predicting collective opinion formation in a population in connection with individual attitudes and their mutual influence is a question of major interest in social sciences [13].

There are two different methods of studying opinion formation in social networks, one based on Bayesian learning, and the other based on setting mechanisms by which individuals update their attitudes as a result of social interaction [3]. The Bayesian learning approach assumes that individuals update their opinions optimally according to Bayes' theorem as more information about the underlying state of the world becomes available [2]. Although mathematically tractable, Bayesian updating requires some unrealistic assumptions about individuals' knowledge and reasoning ability, and becomes computationally infeasible in complex settings [3, 35]. While non-Bayesian models do not suffer these problems and may yield more accurate approximations to the collective behaviour of a popplulation, there is a high degree of arbitariness in the choice of specific models and parameters to use, which sometimes leads to markedly different results [3, 64].

For the non-Bayesian approach to studying opinion formation, a substantial amount of work uses models and tools from statistical physics [13]. A major theme in statistical physics is how global properties can emerge from local rules, which is similar to the question in social sciences of how the collective opinion of a population evolves as the result of individual attitudes and their mutual influence [40]. In the framework of statistical physics, three possible final states have been identified: (i) the population reaches a *consensus*, meaning that all agents hold the same opinion; (ii) two distinct opinions persist, which is called *polarisation*; or (iii) a state of *fragmentation* appears, where there are more than two different opinions [13]. Some notable statistical physics models of opinion formation include the voter model [15, 32], majority rule models [28], models based on social impact theory [45, 55], the Sznajd model [67, 68], and bounded confidence models [18, 31, 42, 71].

Bounded confidence models, first introduced by Deffuant *et al.* [18, 72] and Hegselmann and Krause [31, 42], capture the notion of a tolerance threshold based on experimental social psychology [74]. Bounded confidence reflects the concept of selective exposure in psychology, which refers to people's tendancy to favour information that supports their views while neglecting conflicting arguments [50, 66]. Both the Deffuant model and the Hegselmann-Krause model consider a set of agents that hold continuous opinions from a real interval. Agents are connected by an interaction network, and neighbouring agents adjust their opinions at discrete time steps whenever their opinions are sufficiently close. The two models mainly differ in their communication regime. In the Deffuant model, a pair of neighbouring agents are selected uniformly at random at each time step, and they

make a compromise towards each other's opinion if and only if their opinion difference is less than a given threshold. ln the Hegselmann-Krause model, agents interact with all of their compatible neighbours simultaneously at each time step and updates their opinions to agree with the average of these neighbours'. The Deffuant model is constructed to study the opinion formation process in large populations, where people interact in small groups such as pairs. By comparison, the Hegselmann-Krause model is suitable for investigating the effect of meetings participated by many people at the same time on the opinion dynamics.

In contrast to the synchronous updating rule of the Hegselmann-Krause model, one can tune the speed at which opinions converge in the Deffuant model through an additional parameter that describes the population's openness to compromises, sometimes referred to as the *cautiousness parameter*. For this reason, we focus on the Deffuant model in this project. Two questions have drawn considerable interest in the study of the Deffuant model, namely, what parameter space gives rise to a final state of consensus, polarisation, or fragmentation, and how long does a system reach the final state [18, 43, 46, 72, 73].

Despite its conciseness, the Deffuant model is not analytically solvable in general, and most results are derived through Monte Carlo simulations. In the final state of the Deffuant model, two opinions are either the same or differ by at least the confidence bound so that no more dynamics can occur. In principle, opinions converge at infinitely long times, as the opinion space is continuous and the difference between opinions becomes arbitrarily small without reaching the same value in finite time unless compromise takes the form of averaging opinions [43]. However, the emergence of the final state is evident at finite values of time as consecutive opinion cliques must be separated far enough so that the cliques will not merge together. Thus, a convergence criterion on the maximum range of opinions within each clique is generally set in numerical simulations.

There have also been efforts to study the Deffuant model from an analytical perspective, using a density function that determines the agents' density in the opinion space [10, 46]. This approach adopts a classical strategy in statistical physics by deriving a rate equation (also called a 'master equation') and can be interpreted as taking the infinite limit of the number of agents [48]. While these derivations do not lead to analytical solutions of the Deffuant model directly, they only require numerical integration, which is faster than running Monte Carlo simulations. However, such density-based method requires some assumptions, such as homogeneous mixing and averaging interacting agents' opinions as the means of compromise.

The Deffuant model also has limitations, and numerous efforts have been made to extend the Deffuant model in order to better reflect reality. For instance, the confidence bound imposes a clear boundary on interacting agents' decision whether or not to adjust their opinions. A small change in the difference between their opinions may lead to a different decision being made. For this reason, smooth confidence bounds have been proposed, with which the attraction of agents decreases as their opinion difference increases [19, 20]. Other generalisations of confidence bound include introducing heterogeneous tolerance thresholds in a population [72, 74] and considering time-dependent thresholds [72]. In addition, the Deffuant model can be naturally extended to vector-valued opinions, which only requires redefining opinion distance [25].

Even with numerical simulations, determining the specific parameters to use for the

confidence bound and openness of mind of a population is an open question for many applications. Studies of variants of the Deffuant model often compare new results with those of the original model. However, numerical simulations of the original model are usually ad hoc and performed for specific networks. Moreover, conclusions are often drawn based on graphic patterns and sometimes rely on simplifying assumptions. We are motivated by such existing results to investigate the Deffuant model on networks in a systematic manner. In particular, we explore the dependence of convergence time and the number of opinion cliques in the final state on network topology, confidence bound, the number of participating agents, and their openness of mind. We first design an algorithm for simulating the Deffuant model on networks, checking the convergence of opinions, and determining the number of opinion cliques in the final state. We then conduct regression analysis to model convergence time as a function of the parameters considered and study the behaviour of opinion cliques in the final state qualitatively. The Deffuant model is an example of a discrete-time repeated game, played pair-wise among a group of agents, which are called *players* in game theory [27, 35, 36]. The game is played until the players' opinions converge. We study the Deffuant model on networks in a game-theoretic framework in the rest of the report.

The networks that we study fall into two categories. The first group consists of complete graphs, cycles, and annular lattices, all of which have deterministic structures. We use simulation results on these networks to compare with those on more complex strucures. In addition, complete graphs can be used to model small communities, where everyone knows each other, such as Rhodes Scholars[1] in a particular year, the inhabitants of a village, and high-level political leaders in a country. Furthermore, large social networks often consist of communities, within which individuals are more closely connected with each other than with outsiders, and complete graphs are sometimes used as approximations to such communities [51]. The second group of networks are random graphs, including cycles and annular lattices with random edges and random graphs generated by the Erdős-Rényi model [30]. These graphs possess some properties that social networks often exhibit. For example, cycles and annular lattices with random edges are a version of the Watts-Strogatz model [53] with original connectivity 2 and 3 respectively. The Watts-Strogatz model captures two properties that are commonly observed in real social networks, which are high clustering, meaning that individuals with mutual friends tend to be friends as well, and short average path lengths [52]. The Erdős-Rényi model is one of the best studied models of network and has been used to study the Deffuant model in previous literature [5, 24, 40, 41, 52].

The rest of this report is organised as follows. In Chapter 2, we introduce relevant definitions from network science, define the Deffuant model in mathematical terms, and present some important known results for the Deffuant model on networks. Chapter 3 describes our methodology and introduces the networks that we use in numerical simulations as well as the numerical approach used for simulations. Chapter 4 presents our original work on the behaviour of the Deffuant model for various networks using numerical simulations and regression analysis. In particular, we explore the dependence of convergence time and the number of opinion cliques in the final state on network structure, confidence

---

[1]The Rhodes Scholarship, named after Cecil John Rhodes, is an international postgraduate award for non-British students to study at the University of Oxford.

bound, the number of participating players, and their willingness to change their minds. In Chapter 5, we summarise our results, and we also discuss the implications for sociology and game theory.

2   Background

In this chapter, we first introduce relevant definitions from network science, then define the Deffuant model, giving some intuition of its design, and finally present some important known results of the Deffuant model on networks.

2.1   Networks

A *network* is, in its simplest form, a set of items (called *nodes*) with connections (called *edges*) between them [52]. Network science is an academic field that uses such abstract frameworks to study the pattern of connections between components of a complex system and the dynamical processes thereon [16, 59]. The advancement of network science has contributed to new discoveries in a wide range of domains, such as biology, ecology, engineering, computer science, and social sciences [8, 9, 11, 16, 35, 52, 69]. According to the social network paradigm in social sciences: *social life consists of the flow and exchange of norms, values, ideas, and other social and cultural resources channeled through a social network* [76]. Therefore, networks provide a natural framework for studying collective social phenomena such as the diffusion of technological innovations, the spread of epidemic diseases, and, relevant to our interests, the formation of opinions in communities.

A subset of ideas in network science originate from graph theory, and we introduce some definitions here, based on [52] and [75], that are relevant for our study.

Definition 1. A *graph G* is a triple consisting of a *node set $V(G)$*, an *edge set $E(G)$*, and a relation that associates with each edge two nodes (not necessarily distinct) called its *endpoints*. A *network* in its simplest form is a graph.

Definition 2. Two nodes are *adjacent* and are *neighbours* if and only if there exists an edge between them.

Definition 3. The *degree* of a node is defined as the number of neighbours it has (i.e. the number of edges connected to the node). A *regular graph* is a graph where each node has the same degree.

Definition 4. *Random-graph models* are probability distributions on graphs of which some specific set of parameters take fixed values, but the networks are random in other aspects.

In the framework of network science, the players in the Deffuant model are represented by nodes of a network, and the pair of players on a randomly selected edge can interact with each other. In the next section, we will give the definition of the Deffuant model and some intuition of its design.

2.2   The Deffuant model

In the model proposed by Deffuant *et al.* [18], randomly selected neighbouring players interact pairwise and make a compromise toward each other's opinion whenever their opinion difference is less than a given threshold.

Definition 5.   Consider a population of N players, the acquaintance of whom is represented by a network G. Let $[a,b] \in \mathbb{R}$ be the opinion space. Suppose that each player i holds a time-dependent opinion $x_i(t) \in [a,b]$ for $t \in \mathbb{N}$, where $\mathbb{N} = \{0,1,2,\cdots\}$. Given an initial profile $\vec{x}(0) \in [a,b]^N$, a *confidence bound* $c \in [0,b-a]$, and a *multiplier* $m \in (0,0.5]$, the *Deffuant model* is the random process $(\vec{x}(t))_{t \geq 0}$ defined as follows: at time t, a pair of neighbouring players i and $j \neq i$, which are selected uniformly at random, update their opinions according to the equations

$$
\begin{aligned}
x_i(t+1) &= \begin{cases} x_i(t) + m\left[x_j(t) - x_i(t)\right], & \text{if } |x_i(t) - x_j(t)| < c, \\ x_i(t), & \text{otherwise}, \end{cases} \\
x_j(t+1) &= \begin{cases} x_j(t) + m\left[x_i(t) - x_j(t)\right], & \text{if } |x_i(t) - x_j(t)| < c, \\ x_j(t), & \text{otherwise}. \end{cases}
\end{aligned}
\tag{2.1}
$$

The Deffuant model adopts a continuous opinion space, as an individual's stance on a specific matter can vary smoothly from one extreme to the other in many real-world scenarios [13]. For instance, one's political position is often not absolutely left or right but somewhere between the two extremes. The study of opinion formation processes traditionally considered an opinion to be a discrete variable, which is a reasonable assumption for some applications. For example, the voter model [15, 32] considers a binary variable that specifies one's decision in a vote.

As in the original paper [18] that introduced the Deffuant model, most later studies treat the initial opinions as being independent and identically distributed according to the uniform distribution on the opinion space $[a,b]$. We also adopt this convention in this report, as our goal is to explore the basic version of the Deffuant model in a systematic manner and provide a point of reference for the results of the model's variants. Nonuniform initial opinion distributions are considered, for example, in [37].

The confidence bound c characterises a population's tolerance of diverse viewpoints. If the opinion difference between a pair of players is smaller than this threshold, then they reduce their disagreement by making a compromise. Otherwise, the two players refuse to discuss and keep their current opinions. In the extreme case of $c = 0$, no iteration leads to compromise, and the initial opinion profile is a fixed point. On the other hand, if $c = b - a$, then any pair of randomly selected neighbouring players make convergent adjustments of their opinions.

The multiplier m, also referred to as a *convergence parameter* in some literature, specifies a population's cautiousness while making compromises. A larger value of m indicates that the poplulation is more willing to make convergent adjustments of their opinions. In the special case of $m = 0.5$, pairs of interacting players agree on the average of their opinions whenever their opinion difference is less than the confidence bound c.

The Deffuant model, in its original form [18], considers the confidence bound and the multiplier to be constant in time and across the whole population. In such setting, the average opinion of a pair of players is preserved before and after their interaction. Hence, if initial opinions are independent and identically distributed according to the uniform distribution on the opinion space $[0,1]$, the expected mean opinion of the population is always 0.5.

Convergence of opinions is generally defined as the appearance of a stable configuration where no more dynamics can occur. In a final state, the opinion distribution is a superposition of Dirac delta functions in the opinion space $[a,b]$, such that consecutive spikes are separated by at least c. We call the group of players that share the same opinion as a *clique*. Any two players in the final state either are in the same clique or hold opinions that differ by at least c. We use the notation $K \in \mathbb{N}$ to denote the number of opinion cliques in a final state.

2.3 The Deffuant model on various networks

To the best of our knowledge, the Deffuant model has been studied on only a small subset of networks, which include complete graphs, two-dimensional grids, Erdős-Rényi random graphs, Watts-Strogatz random graphs, and Barabási-Albert random graphs [7]. The Barabási-Albert model is a simple model that generates random networks that have power-law degree distributions, which are widely observed in natural and artificial systems such as the World Wide Web, citation networks, and some social networks [52].

Many papers study the Deffuant model on complete graphs, which allow any pair of players to interact [18]. For this homogeneous mixing case, the population's opinions always converge to a final state [46]. It has been shown that a large confidence bound, c, gives rise to a final state of consensus, while multiple opinion cliques can persist for small values of c [18, 24, 43, 72, 73]. The same phenomena were observed in simulations on two-dimensional grids in the form of square lattices, Erdős-Rényi random graphs, Watts-Strogatz random graphs, and Barabási-Albert random graphs [18, 40, 41, 65]. Moreover, a conjecture based on numerical simulations on complete graphs states that the number of opinion cliques in the final state, K, is inversely proportional to c [18, 72, 73]. Numerical simulations on complete graphs also suggest that multiplier, m, and the number of participating players, N, have no effect on K [18, 72]. However, a later study, also based on numerical simulations, observes that the number of major opinion cliques which contain many players is a function of c, whereas the number of minor opinion cliques (sometimes referred to as *minorities*) depends on m [43].

The Deffuant model on two-dimensional grids, Watts-Strogatz random graphs, and Barabási-Albert random graphs also exhibits behaviour that is different from the homogeneous mixing case. For instance, simulations on square lattices and Barabási-Albert random graphs suggest that K depends not only on c but also on N when multiple opinion cliques persist in the final state [18, 65]. Simulations on Watts-Strogatz random graphs indicate that K is a function of c and the network structual disorder, and the presence of disorder only affects the convergence time, T, slightly [29]. Such results further motivate us to study the convergence time carefully.

Existing research of the Deffuant model on Erdős-Rényi random graphs has mainly focused on adaptive networks that evolve with the game [40, 41]. For Watts-Strogatz random graphs, the study of the model has centred around the opinion cliques in the final state so far [29]. For these reasons, we shall study complete graphs, cycles, annular lattices, cycles and annular lattices with random edges, and Erdős-Rényi random graphs. The first three networks have deterministic structures, which provide results for comparison with those of the three random graphs.

3 Methods

In this chapter, we describe our methodology for exploring the Deffuant model on various network structures, introduce the networks that we study, and describe our approach for performing numerical simulations in detail.

3.1 Approach

We investigate the Deffuant model on various networks in a systematic manner, as numerical simulations of the original model are usually ad hoc, and conclusions are often drawn based on graphic patterns. For each network structure, we conduct regression analysis to model convergence time as a function of confidence bound, the number of participating players, and their openness of mind represented by a multiplier. We then study the behaviour of opinion cliques in the final state qualitatively, as such approach is more natural than conducting regression analysis due to the more complicated nature of the opinion clique distributions.

3.2 Networks studied

We study the Deffuant model on a range of networks in order to understand the effect of network structure on convergence time and the number of opinion cliques in the final state. Some of the networks that we study have deterministic structures, while others are random graphs. In Table 3.1, we list the notations, definitions, and examples for these networks.

The first group of networks that we study are deterministic graphs, including complete graphs (K_n), cycles (C_n), and annular lattices (A_n). We use simulation results on these networks to compare with those on more complex strucures. In addition, complete graphs can be used to model small communities, where everyone knows each other, and as approximations to communities in large social networks [51].

The second group of networks that we study consists of random graphs, which are cycles with random edges ($C_{n,s}$), annular lattices with random edges ($A_{n,s}$), and random graphs generated by the Erdős-Rényi $G(n, p)$ model. The $G(n, p)$ model is the most fundamental and widely studied random graph ensemble and is often used in the study of social networks [52]. Nevertheless, the Erdős-Rényi $G(n, p)$ model does not generate local clustering which has been observed in numerous social networks. The Watts-Strogatz model produces random graphs with local clustering, which is commonly observed in real social networks [53, 52]. The random graphs that are generated by the Watts-Strogatz model also have short average path lengths, which is another property that are common to social networks [52]. Cycles and annular lattices with randomly generated extra edges are a version of the Watts-Strogatz model with original connectivity 2 and 3, respectively. The Watts-Strogatz model actually has two versions, with one rewiring edges of the existing graph

and the other one adding random edges to the existing graph [53, 70]. These two versions of the model have similar behaviour when the proportion of random edges is small [52]. The cycles and annular lattices with random edges that we consider in this report belong to the second version of the Watts-Strogatz model.
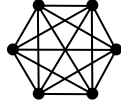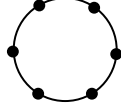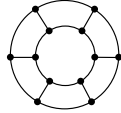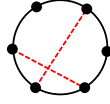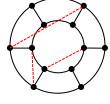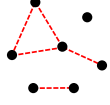
Network	Definition	Example
K_n	A *complete graph* K_n has n pairwise adjacent nodes [75].	
C_n	For $n \geq 3$, a *cycle* C_n has node set $\{v_j \mid 1 \leq j \leq n\}$ and edge set $\{v_j v_{j+1} \mid 1 \leq j \leq n-1\} \cup \{v_n v_1\}$ [75].	
A_n	For even n, we define an *annular lattice* A_n as two cycles $C_{n/2}$ joined together by $\frac{n}{2}$ edges.	
$C_{n,s}$	For $n \geq 3$ and $0 < s < \frac{n-3}{n-1}$, we define $C_{n,s}$ as follows: add an edge between a pair of non-adjacent nodes uniformly at random on C_n, and repeat this process sN times in order to add sN distinct extra edges on the cycle C_n.	
$A_{n,s}$	For even $n \geq 4$ and $0 < s < \frac{n-4}{n-1}$, we define $A_{n,s}$ as follows: add an edge between a pair of non-adjacent nodes uniformly at random on A_n, and repeat this process sN times in order to add sN distinct extra edges on the annular lattice A_n.	
$G(n,p)$	For $n \in \mathbb{Z}_{>0}$ and $p \in [0,1]$, random graphs are generated from the Erdős-Rényi $G(n,p)$ model [30] as follows: start with n disconnected nodes and place an edge between each distinct pair with independent probability p.	

Table 3.1: Summary of the definitions of the networks on which we study the Deffuant model. In each example network, black solid lines denote deterministic edges, and red dashed lines represent edges that are generated randomly.

3.3   Simulations

Without loss of generality, we consider the Deffuant model on the opinion space $[0,1]$. In other words, we normalise the dynamical game so that each player's opinion is between 0 and 1 at any time step. We can generalise our results to any closed real interval by linear transformation, but we lose no generality by assuming an opinion space $[0,1]$. In addition, we allow the multiplier m to be any number in the interval $(0,1)$, as compared with the interval $(0,0.5]$ considered by the original model [18]. This generalisation is useful as interacting players could possibly be convinced to believe in others' opinions more than their own. Moreover, considering $m \in (0,1)$ reveals interesting phenomena that we will discuss in Chapter 4.

Table 3.2 lists the values for the number of participating players (N), confidence bound (c), and multiplier (m) that we consider in our simulations. This set of parameter values provides a reasonably fine mesh of the underlying parameter space, which provides sufficiently many data points for our regression analysis. However, the specific parameter values considered are completely arbitrary choices except for $c = 1$ and $m = 0.5$. For $c = 1$, any pair of randomly selected players make convergent opinion adjustments, which corresponds to interaction without confidence bound. For $m = 0.5$, each pair of randomly selected players agree on the average of their opinions whenever their opinion difference is below c. Theoretically, there is no upper bound on the number of players that one can consider in a population, but running numerical simulations on extremely large populations is computationally unrealistic. Hence, we set $N = 1000$ as an upper bound for our simulations, and the behaviour of the model with larger population size can be deduced from the regression models that we construct.

N	10, 50, 100, 200, 300, 400, 500, 600, 700, 800, 900, 1000
c	0.1, 0.2, 0.3, 0.4, 0.5, 0.6, 0.7, 0.8, 0.9, 1
m	0.1, 0.2, 0.3, 0.4, 0.5, 0.6, 0.7, 0.8, 0.9

Table 3.2: Values of the number of players (N), confidence bound (c), and multiplier (m) that we consider in our simulations.

In principle, the convergence time, T, and the number of opinion cliques in the final state, K, are both unpredictable, as the initial opinion profile, the pair of players that interact at each time step, and the graphs generated by random graph ensembles are all stochastic. In order to smooth these noises, we run 10 groups of independent simulations for each network (introduced in Section 3.2) and each combination of N, c, and m considered. For each simulation, we first generate a group of N independent and identically distributed initial opinions according to a uniform distribution on $[0,1]$. We then play the game according to the Deffuant model.

Theoretically, opinions converge to one or multiple values in the final state, but this is in principle achieved at infinitely long times, as the opinion space is continuous and opinions approach each other arbitarily close without reaching the same value in finite times unless $m = 0.5$ [43]. However, the emergence of the final state is evident at finite times as

consecutive opinion cliques must be separated by a distance of at least c so that the two cliques will not merge together. The smaller the confidence bound, the larger the maximum number of opinion cliques that can form in the final state. The smallest confidence bound that we consider is $c = 0.1$, which can give rise to at most $K = 11$ different opinions in the final state, with consecutive values separated by 0.1. Thus, a maximum range of 0.02 within each opinion clique is a reasonable approximation for the purpose of numerical simulations. We design a code in PYTHON that checks the convergence of opinions automatically. We present a pseudocode in Algorithm 1 to illustrate our design of the simulations. Based on some test simulations, we choose to set a bailout time of 10^9 (time steps) for each simulation in order to balance the trade-off between the number of simulations that are expected to finish before the cutoff time and the time frame of the project. For every 10 (denoted by t_0 in Algorithm 1) time steps, we check if the opinions have converged to one or multiple cliques, within which the range of opinions is at most 0.02 (denoted by δ in Algorithm 1).

If the opinions have converged by the bailout time, then we record the convergence time (T) and the number of opinion cliques (K). Otherwise, we record $T = 3.55 \times 10^9$, a strict upper bound that is higher than all possible convergence times. In Chapter 4, we use the natural logarithm of T in some plots as T varies across different levels of magnitude depending on the network structure, confidence bound, and multiplier under consideration. The maximum convergence time can be the bailout time, 10^9, which would give $\ln(10^9) \approx 21$. For comparison, $\ln(3.55 \times 10^9) \approx 22$ differentiates simulations that did not converge by the the bailout time in the plots.

Algorithm 1 Algorithm for simulating the Deffuant model on networks

---

Input: $G \leftarrow$ network
        $N \leftarrow$ number of players
        $c \leftarrow$ confidence bound
        $m \leftarrow$ multiplier
        $t_0 \leftarrow$ accuracy
        $\delta \leftarrow$ tolerence
        $t_b \leftarrow$ bailout time
Output: $T \leftarrow$ convergence time
        $K \leftarrow$ number of opinion cliques

1: **for** $k = 1$ to N **do**
2:    $x_k(0) \leftarrow \text{UNIFORM}([0,1])$;
3: **end for**
4: $t \leftarrow 0$;
5: **while** $t < t_b$ **do**
6:    **for** iteration $= 1$ to t_0 **do**
7:       $(i, j) \leftarrow \text{UNIFORM}(\text{EDGES}(G))$;
8:       **if** $|x_i(t) - x_j(t)| < c$ **then**
9:          $x_i(t+1) = x_i(t) + m[x_j(t) - x_i(t)]$;
           $x_j(t+1) = x_j(t) + m[x_i(t) - x_j(t)]$;
10:      **else**
11:        $x_i(t+1) = x_i(t)$;
          $x_j(t+1) = x_j(t)$;
12:      **end if**
13:    **end for**
14:    $t \leftarrow t + t_0$;
15:    y_1 to $y_N \leftarrow \text{SORT}(x_1(t)$ to $x_N(t))$;
16:    $K \leftarrow 0$;
17:    $K_u \leftarrow \lceil (y_N - y_1)/c \rceil + 1$;
18:    **for** clique $= 1$ to K_u **do**
19:      **if** $\text{MAX}(y) - y_1 \leq \delta$ **then**

20:       $T \leftarrow t$;
21:       $K \leftarrow K + 1$;
22:       BREAK;
23:      **else**
24:       $l \leftarrow 1$;
25:       **while** $y_l \leq y_1 + \delta$ **do**
26:         $l \leftarrow l + 1$;
27:       **end while**
28:       **if** $y_l - y_{l-1} < c$ **then**
29:         $K \leftarrow 0$;
30:         BREAK;
31:       **else**
32:         $K \leftarrow K + 1$;
33:         $\text{REMOVE}(y_1$ to $y_{l-1})$;
34:         $\text{RELABEL}(\vec{y})$ starting from 1;
35:       **end if**
36:      **end if**
37:      **if** clique $= K_u$ and $\{y\} \neq \varnothing$ **then**
38:       $K \leftarrow 0$;
39:      **end if**
40:    **end for**
41:    **if** $K > 0$ **then**
42:      $T \leftarrow t$;
43:      BREAK;
44:    **end if**
45: **end while**
46: **if** $T = t_b$ and $K = 0$ **then**
47:    $T \leftarrow 3.55 \times t_b$;
     $K \leftarrow \text{N/A}$;
48: **end if**

---

4 Numerical simulations on deterministic and random networks

In this chapter, we study the Deffuant model on various deterministic and randomly generated networks by considering different network structures and interaction mechanisms between pairs of players. For each network structure, we first use linear regression analysis to model convergence time (T) as a function of the number of participating players (N), confidence bound (c), and multiplier (m). We then comment on the phenomena that we observed about the number of opinion cliques in the final state qualitatively.

For the linear regression analysis, we adopt the method of ordinary least squares, as the estimator is unbiased and consistent if the errors have the same finite variance and are uncorrelated with the regressors [26]. If the errors are also normally distributed, ordinary least squares is the maximum likelihood estimator [26]. We check these assumptions throughout our model selection process.

For robust regression analysis, we only use simulation results for cases when there are 100 or more players in the network in order to reduce the stochasticity introduced by the random initial opinion distribution. In addition, sociologists are often interested in the opinion dynamics of large populations, which also justifies our choice. Furthermore, for all cases considered, we run 10 different simulations and take the average, in order to mitigate the influence of the random initial opinion distribution and the order in which pairs of players are selected randomly.

4.1 Complete graphs

The Deffuant model, in its simplest form [18], allows any pair of players in the system to interact, which is equivalent to studying the model on complete graphs. Complete graphs can be used to model small communities, where everyone knows each other, and as approximations to communities in large social networks [51].

Figure 4.1 summarises the values of $\ln(T)$ observed in simulations for which $N = 10$, 50, 100, 200, 400, 600, 800, and 1000, as these are representative of the trends that we observe in all simulations. We take the natural logarithm of T for the sake of revealing patterns in the change of the colours. We present the same subset of plots for other network structures in the rest of Chapter 4 for the same reason.

We start our analysis with some data exploration in order to get an intuition of the potential relationship between the response, T, and the explanatory variables, N, c, and m. We also conduct data exploration for all other netwosks but only give full details here, as the process is similar. Scatter plots shown in Figure 4.2 suggest dependence of T on N, c, and possibly m. In particular, the relationship between T and c undergoes a transition at $c = 0.5$, below which we observe a larger variation of T. Figures 4.3 and 4.4 give the scatter plots that correspond to $c < 0.5$ and $c \geq 0.5$ respectively. Since Figures 4.3 and 4.4
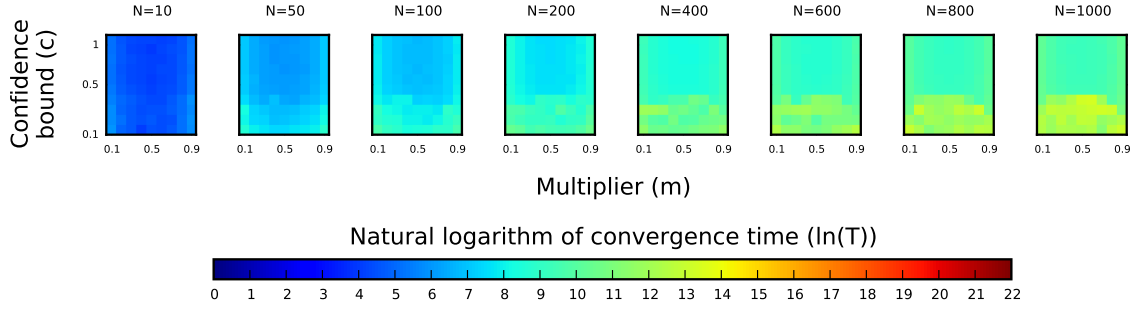
Figure 4.1: Summary of convergence time of simulations on complete graphs for $N = 10$, 50, 100, 200, 400, 600, 800, and 1000. These are representative of the trends that we observe in all simulations. This and all subsequent figures of this type are generated using the MATPLOTLIB library for Python developed by J. D. Hunter [33].

show qualitatively distinct behaviour for $c < 0.5$ and $c \geq 0.5$, we shall consider distinct models for each case.

Figure 4.2: Scatter plots for convergence time (T) on complete graphs against the number of players (N), confidence bound (c), and multiplier (m). The figure is drawn using the software environment R [60].

4.1.1 Convergence time

The case of $c < 0.5$

We start by fitting a normal linear model given by the equation

$$T = \beta_0 + \beta_1 N + \beta_2 N^2 + \beta_3 c + \beta_4 c^2 + \beta_5 m + \beta_6 m^2 + \beta_7 mc + \beta_8 Nc + \beta_9 Nm + \varepsilon, \quad (4.1)$$

where β_j ($j = 0, 1 \cdots, 9$) are coefficients to be estimated and ε is assumed to be an independent and normally distributed error with zero mean and constant variance for every observation. The model given by Equation 4.1 is a linear model because it is linear with respect to the coeffcients β_j ($j = 0, 1 \cdots, 9$). We include all the explanatory variables up to
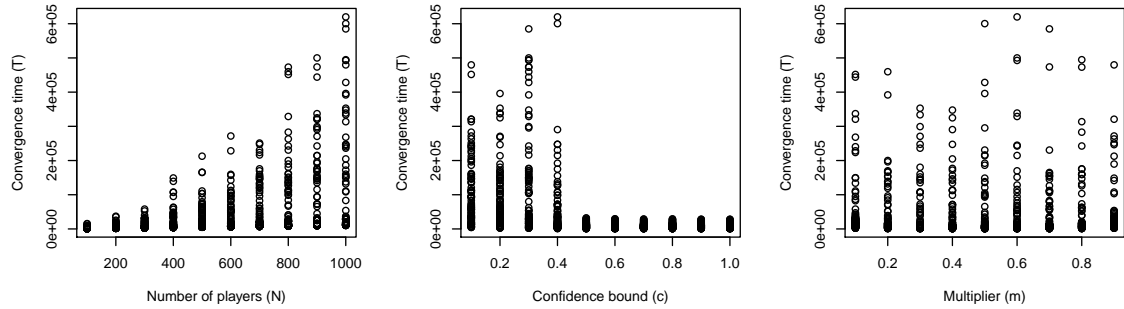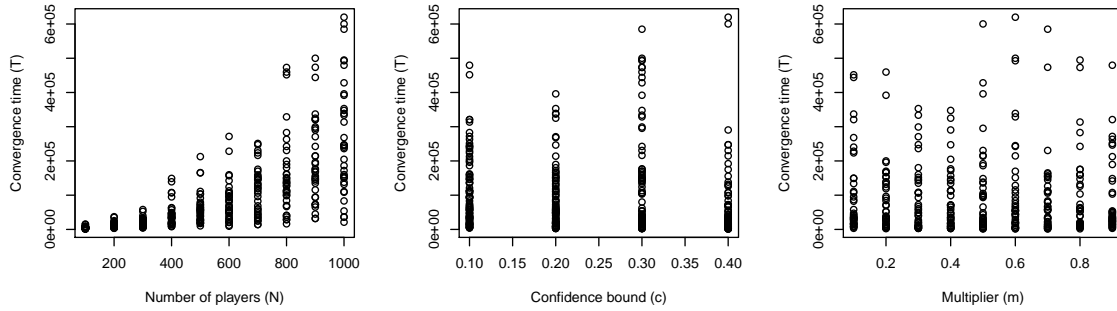
Figure 4.3: Scatter plots for convergence time (T) against the number of players (N), confidence bound (c), and multiplier (m), using simulation results on complete graphs for which $c < 0.5$. The figure is drawn using the software environment R [60].

Figure 4.4: Scatter plots for convergence time (T) against the number of players (N), confidence bound (c), and multiplier (m), using simulation results on complete graphs for which $c \geq 0.5$. The figure is drawn using the software environment R [60].
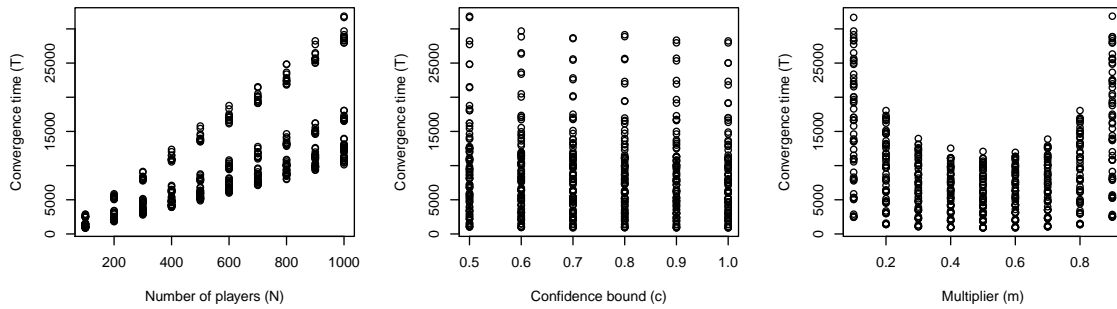
the second order in the full model (Equation 4.1) to account for the curvature observed in Figure 4.3. We will drop statistically insignificant variables during model reduction.

Before proceeding with model selection, we check the validity of the model assumptions. Subfigure 4.5a checks the assumption that the errors have zero mean and constant variance by plotting studentised residuals against response values predicted by Equation 4.1. Ideally, variance should be constant in the vertical direction and the scatter should be symmetric vertically about 0. However, Subfigure 4.5a indicates that the assumption of constant variance does not hold as the points follow a clear wedge-shaped pattern, with the vertical spread of the points increasing with the fitted values. Subfigure 4.5b checks the assumption of normality by plotting the sample quantiles against the quantiles of a normal distribution. Data generated from a normal distribution should follow the 45° line through the origin closely, but the Q-Q plot in Subfigure 4.5b suggests non-normality of the residuals. The diagonostics show the necessity of stabilising variance and making the data more normal distribution-like.

The one-parameter Box-Cox method [12] is a popular way to determine a transforma-
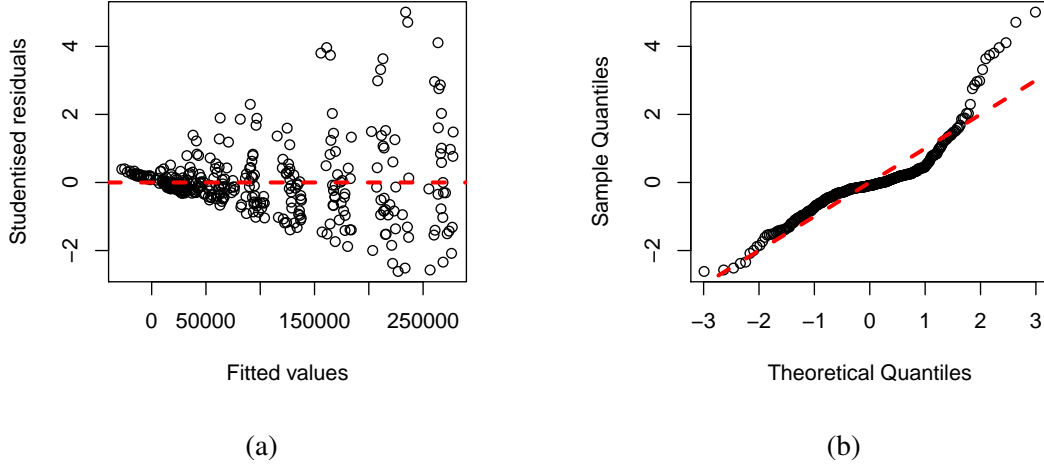
(a)   (b)

Figure 4.5: (a) Studentised residuals against fitted values and (b) normal Q-Q plot of studentised residuals for Equation (4.1) using simulation results on complete graphs for which $c < 0.5$. In (a), the red reference dashed line is the horizontal line through the origin. Ideally, variance should be constant in the vertical direction and the scatter should be symmetric vertically about 0. In (b), the red reference dashed line is the 45° line through the origin. Data generated from a normal distribution should follow the red dashed line closely. The figure is drawn using the software environment R [60].

tion on strictly positive responses [56]. A Box-Cox transformation maps the response T to $T^{(\lambda)}$, where the family of transformations indexed by λ is defined by

$$T^{(\lambda)} = \begin{cases} \frac{T^{\lambda}-1}{\lambda} & \text{if } \lambda \neq 0, \\ \ln(T) & \text{if } \lambda = 0. \end{cases} \tag{4.2}$$

Figure 4.6 shows that the confidence interval for λ at the 95% confidence level runs roughly from -0.1 to 0. We choose to set $\lambda = 0$, as this corresponds to taking a natural logarithm. The diagonostics of the new model indicate that we do log-transformation again, which gives the model

$$\ln(\ln(T)) = \beta_0 + \beta_1 N + \beta_2 N^2 + \beta_3 c + \beta_4 c^2 + \beta_5 m + \beta_6 m^2 + \beta_7 mc + \beta_8 Nc + \beta_9 Nm + \varepsilon, \tag{4.3}$$

where ε is assumed to be an independent and normally distributed error with zero mean and constant variance for every observation. The variance for ε is not necessarily the same for Equations (4.1) and (4.3). We use the same notation for ε in the rest of the report, with the understanding that it is of course different for each model.

This time, Subfigure 4.7a shows approximately constant variance in the vertical direction and the scatter is roughly symmetric vertically about 0. There are no studentised residuals outside the $[-3,3]$ range, which implies that there are no serious outliers. In Subfigure 4.7b, the points follow the 45° line through the origin closely. The diagnostic plots show that our model assumptions are reasonable for Equation (4.3).
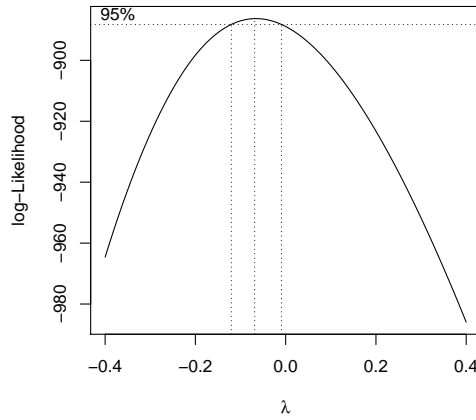
Figure 4.6: Profile log-likelihood plot for parameter λ of the Box-Cox transformation. The figure is drawn using the software environment R [60].
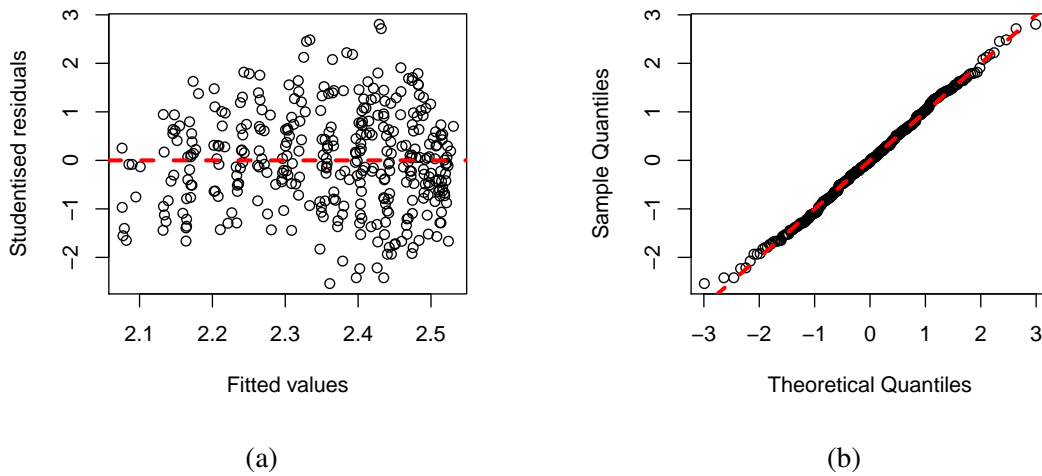
Figure 4.7: (a) Studentised residuals against fitted values and (b) normal Q-Q plot of studentised residuals for Equation (4.3) using simulation results on complete graphs for which $c < 0.5$. The red reference dashed lines in (a) and (b) are the horizontal line through the origin and the $45°$ line through the origin respectively. The diagnostic plots show that our model assumptions of normally distributed errors with zero mean and constant variance are reasonable for Equation (4.3). The figure is drawn using the software environment R [60].

Proceeding with model selection, we use the Akaike Information Criterion (AIC) [4] to select the 'best' subset of predictors, as the method balances the trade-off between the goodness of fit and the complexity of a model. This model selection approach aims to

minimise AIC which is defined by

$$\text{AIC} = 2(p - \ln(L)), \tag{4.4}$$

where p is the number of estimated parameters and L is the maximum value of the likelihood function for the model. AIC-based model selection drops the first-order term of c and all terms that include m, giving the model

$$\ln(\ln(T)) = \beta_0 + \beta_1 N + \beta_2 N^2 + \beta_3 c^2 + \beta_4 Nc + \varepsilon. \tag{4.5}$$

The diagnostic graphs of Equation (4.5) are similar to those in Figure 4.7 and are therefore acceptable.

Cook's distance [17] measures the influence of a data point in a least squares regression analysis. A commonly used threshold for detecting highly influential observations is $8/(n - 2p)$, where n is the number of observations and p is the number of fitted parameters [54]. Figure 4.8 reveals 3 influential observations. We remove these 3 points and give the estimates for the coefficients β_j ($j = 0, 1, \cdots, 4$) of Equation (4.5) in Table 4.1, accurate to 4 significant figures using scientific notation. Table 4.1 is part of the regression output given by the software environment R [60]. The column of t value gives the values of the t-statistic for the hypothesis test with the null hypothesis that the corresponding regression coefficient is 0. The column of $\Pr(> |t|)$ gives the probability for a test statistic to be at least as extreme as the observed t value if the null hypothesis were true. A low value of $\Pr(> |t|)$ suggests that it would be rare to get a result as extreme as the observed value if the coefficient under consideration were 0, and hence we should keep the corresponding term in our model.

	Estimate	Std. Error	t value	$\Pr(> |t|)$
β_0	2.139	1.380×10^{-2}	1.550×10^2	$< 2 \times 10^{-16}$
β_1	7.124×10^{-4}	5.255×10^{-5}	1.356×10	$< 2 \times 10^{-16}$
β_2	-3.763×10^{-7}	4.178×10^{-8}	-9.006	$< 2 \times 10^{-16}$
β_3	-9.922×10^{-1}	1.076×10^{-1}	-9.220	$< 2 \times 10^{-16}$
β_4	3.696×10^{-4}	8.983×10^{-5}	4.114	4.850×10^{-5}

Table 4.1: Summary of regression parameters for Equation (4.5), accurate to 4 significant figures using scientific notation.

The coefficient of determination, $R^2 \in [0, 1]$, is a measure of goodness of fit of a regression model [22]. Values of R^2 that are closer to 1 indicate better fits. An $R^2 = 0$ implies that the dependent variable cannot be predicted from the independent variable, and an $R^2 = 1$ means that the dependent variable can be predicted without error from the independent variable. Let $\hat{T}_i$ be the predicted value for the observed convergence time T_i ($i = 1, 2, \cdots, n$), and let $\bar{T} = (\sum_{i=1}^{n} T_i)/n$. The definition of R^2 is given by

$$R^2 = \frac{\sum_{i=1}^{n} (\hat{T}_i - \bar{T})^2}{\sum_{i=1}^{n} (T_i - \bar{T})^2}. \tag{4.6}$$
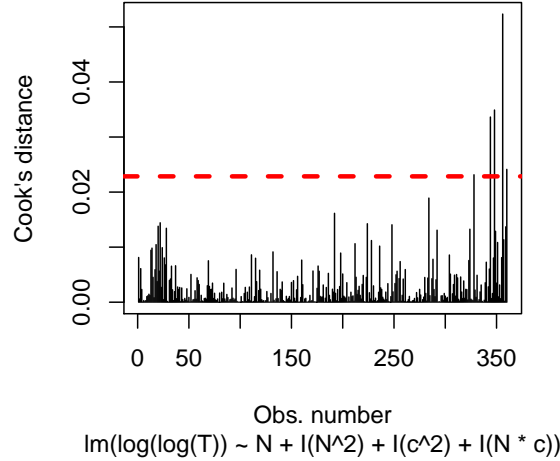
Figure 4.8: Cook's distances for the model defined by Equation (4.5). The red dashed line is a horizontal line through $8/(n-2p)$, where n is the number of observations and p is the number of fitted parameters. This line gives the threshold for detecting highly influential observations that are particularly worth checking for validity. The figure is drawn using the software environment R [60].

Table 4.2 summarises the values of AIC and R^2 of regression models considered for simulations on complete graphs for which $c < 0.5$. The substantial increase in R^2 and decrease in AIC indicate that our final model (Equation (4.5)) has much better goodness of fit and a considerably simpler form than our orignal model (Equation (4.1)).

Model	AIC	R^2
Equation (4.1)	8146.1	0.5272
Equation (4.3)	−2040.4	0.8164
Equation (4.5)	−2037.1	0.8246

Table 4.2: Values of AIC and R^2 of regression models considered for simulations on complete graphs for which $c < 0.5$, accurate to 5 and 4 significant figures, respectively.

The case of $c \geq 0.5$

For $c \geq 0.5$, we go through a similar model selection process to the case of $c < 0.5$ and arrive at the following equation

$$\ln(T) = \beta_0 + \beta_1 \ln(N) + \beta_2 c + \beta_3 c^2 + \beta_4 m + \beta_5 m^2 + \varepsilon. \qquad (4.7)$$

We include an $\ln(N)$ term in the full model (Equation 4.7) to account for the linear dependence of T on N which Figure 4.4 suggests. AIC-based model selection shows

statistical significance of the $\ln(N)$ term. For Equation (4.7), we have AIC ≈ -3248.9 and $R^2 \approx 0.9965$. Table 4.3 gives the estimates for the coefficients β_j ($j = 0, 1, \cdots, 5$) of Equation (4.7), accurate to 4 significant figures using scientific notation.

	Estimate	Std. Error	t value	$\Pr(> |t|)$
β_0	4.024	5.038×10^{-2}	7.988×10	$< 2 \times 10^{-16}$
β_1	1.062	3.039×10^{-3}	3.495×10^2	$< 2 \times 10^{-16}$
β_2	-1.316	1.277×10^{-1}	-1.031×10	$< 2 \times 10^{-16}$
β_3	7.346×10^{-1}	8.472×10^{-2}	8.671	$< 2 \times 10^{-16}$
β_4	-6.261	3.704×10^{-2}	-1.690×10^2	$< 2 \times 10^{-16}$
β_5	6.262	3.612×10^{-2}	1.733×10^2	$< 2 \times 10^{-16}$

Table 4.3: Summary of regression parameters for Equation (4.7), accurate to 4 significant figures using scientific notation.

Table 4.3 suggests combining m and m^2 together as a single term $(m - 0.5)^2$ and c and c^2 as $(c - 1)^2$. The model with combined terms has two fewer coefficients to estimate than Equation (4.7) and very close values of AIC ≈ -3240.9 and $R \approx 0.9964$. Thus, we update our model for $c \geq 0.5$ as the simpler model given by

$$\ln(T) = \beta_0 + \beta_1 \ln(N) + \beta_2 (c - 1)^2 + \beta_3 (m - 0.5)^2 + \varepsilon. \qquad (4.8)$$

Table 4.4 gives the estimates for the coefficients β_j ($j = 0, 1, 2, 3$) of Equation (4.8), accurate to 4 significant figures using scientific notation.

	Estimate	Std. Error	t value	$\Pr(> |t|)$
β_0	1.865	1.916×10^{-2}	9.734×10	$< 2 \times 10^{-16}$
β_1	1.062	3.067×10^{-3}	3.463×10^2	$< 2 \times 10^{-16}$
β_2	4.530×10^{-1}	2.398×10^{-2}	1.889×10	$< 2 \times 10^{-16}$
β_3	6.262	3.646×10^{-2}	1.718×10^2	$< 2 \times 10^{-16}$

Table 4.4: Summary of regression parameters for Equation (4.8), accurate to 4 significant figures using scientific notation.

Summary of convergence time results

Through the above regression analysis, we obtained the models given by Equations (4.5) and (4.8) for complete graphs with confidence bounds $c < 0.5$ and $c \geq 0.5$, respectively. The different forms of these equations confirm our conjecture based on data exploration that convergence time, T, undergoes a transition at $c = 0.5$. To be more precise, the regression results suggest that the behaviour of T differs for $c \leq 0.4$ and $c \geq 0.5$. In order to determine a more precise critical value for c, one should conduct numerical simulations using $c \in (0.4, 0.5)$.

For $c < 0.5$, multiplier m has no statistically significant impact on T, and T increases with N. For $c \geq 0.5$, the effects of N, c, and m on T are independent. In particular, T

increases with N roughly linearly. We also observe that T increases with $(c-1)^2$ exponentially and obtains a minimum at $c = 1$, which corresponds to interaction without confidence bound. In other words, for fixed N and m, convergence time on complete graphs is minimal when any pair of randomly selected players make a convergence compromise. Furthermore, T increases with $(m-0.5)^2$ exponentially and obtains a minimum at $m = 0.5$, in which case each pair of randomly selected players agree at their average opinion whenver their opinion difference is less than the given confidence bound.

4.1.2   The number of opinion cliques

For each combination of N, c, and m, we average the number of opinion cliques in the final state, K, if and only if at least 6 out of the 10 simulations converged within the bailout time, as defined in Section 3.3. Otherwise, we state that division of opinion was observed for such combination of parameters. We use the same standard to decide the number of opinions in the final state in the rest of the report.

Figure 4.9 summarises the number of opinion cliques that emerged in simulations on complete graphs for which $N = 10, 50, 100, 200, 400, 600, 800,$ and 1000.
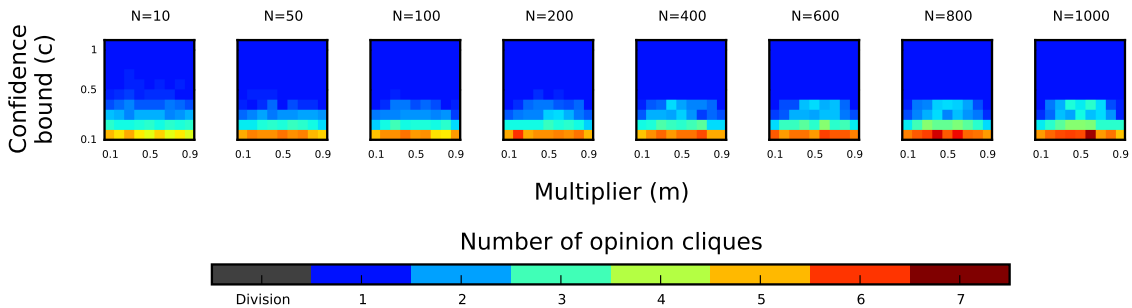
Figure 4.9: Summary of the number of opinion cliques that emerged in simulations on complete graphs for $N = 10, 50, 100, 200, 400, 600, 800,$ and 1000. These are representative of the trends that we observe in all simulations. We use grey colour to represent simulations that did not converge by the bailout time (10^9 time steps).

Figure 4.9 reveals that K depends on the number of participating players, N, only for confidence bound $c < 0.5$, with the most dramatic changes happening in the region of $c = 0.1$. For $c \geq 0.5$, consensus is reached consistently. For $0.2 \leq c \leq 0.4$, K generally increases with N, and $1 \leq K \leq 4$. For $c = 0.1$, we observed that $K \geq 5$ for $N \geq 200$. In addition, for $c < 0.5$ and $N \geq 600$, K is generally larger for m closer to 0.5. This phenomenon is reasonable because, as $m \to 0.5$, players tend to agree with each other and hence have less time to change their opinions. As the convergence time is shortened as $m \to 0.5$, more opinion cliques tend to persist in the final state.

4.2 Cycles

In this section, we explore the behaviour of convergence time and the number of opinion cliques in the final state on cycles. We use simulation results on cycles to compare with those on cycles with random edges.

4.2.1 Convergence time

Figure 4.10 summarises the values of $\ln(T)$ observed in simulations on cycles for which $N = 10, 50, 100, 200, 400, 600, 800,$ and 1000.

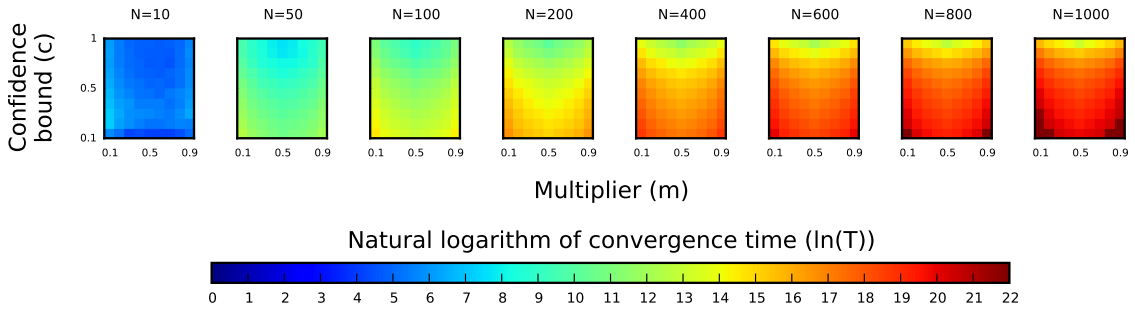Figure 4.10: Summary of convergence time recorded in simulations on cycles for $N = 10$, 50, 100, 200, 400, 600, 800, and 1000.

For large N, $\ln(T)$ changes with m rapidly when c is close to 1. We speculate that a singularity arises at $c = 1$ and $m = 0.5$, as $N \to \infty$. For complete graphs, simulation results suggest that T obtains a global minimum at $c = 1$ and $m = 0.5$ when N is fixed, and that $T \to \infty$ as $N \to \infty$. Linear regression models cannot capture singularity points, so we exclude data points that correspond to $c \geq 0.7$ from our regression analysis for cycles.

Following a similar AIC-based regression selection process as outlined in Section 4.1, we arrive at the model

$$\ln(T) = \beta_0 + \beta_1 \ln(N) + \beta_2 c + \beta_3 c^2 + \beta_4 (m - 0.5)^2 + \beta_5 Nm + \varepsilon. \qquad (4.9)$$

Table 4.5 summarises the estimates for coefficients β_j ($j = 0, 1, \cdots, 5$) of Equation (4.9), accurate to 4 significant figures using scientific notation. Table 4.5 is part of the regression output given by the software environment R [60]. For Equation (4.9), $R^2 \approx 0.9991$ and AIC ≈ -3257.6.

As was true for complete graphs, the convergence time, T, increases as more players are connected on a cycle. However, simulations indicate different behaviour of T in connection with the number of players (N), confidence bound (c), and multiplier (m) for the Deffuant model on cycles. For instance, simulations show no clear transition of the behaviour of T with respect to c. Nevertheless, for values of c that are close to 1, $\ln(T)$ changes with m more rapidly as N increases. In addition, the effects of N and m on T are weakly coupled through a factor $\exp(\beta_5 Nm)$, where β_5 is estimated to be -7.642×10^{-5}.

	Estimate	Std. Error	t value	$\Pr(>|t|)$
β_0	-6.313×10^{-1}	3.054×10^{-2}	-2.067×10	$< 2 \times 10^{-16}$
β_1	3.018	5.142×10^{-3}	5.870×10^{2}	$< 2 \times 10^{-16}$
β_2	-2.630	6.357×10^{-2}	-4.137×10	$< 2 \times 10^{-16}$
β_3	-1.624	7.708×10^{-2}	-2.107×10	$< 2 \times 10^{-16}$
β_4	9.371	4.669×10^{-2}	2.007×10^{2}	$< 2 \times 10^{-16}$
β_5	-7.642×10^{-5}	1.713×10^{-5}	-4.461	9.770×10^{-6}

Table 4.5: Summary of regression parameters for Equation (4.9), accurate to 4 significant figures using scientific notation.

4.2.2   The number of opinion cliques

Figure 4.11 summarises the number of opinion cliques that emerged in simulations on cycles for which $N = 10, 50, 100, 200, 400, 600, 800,$ and 1000.
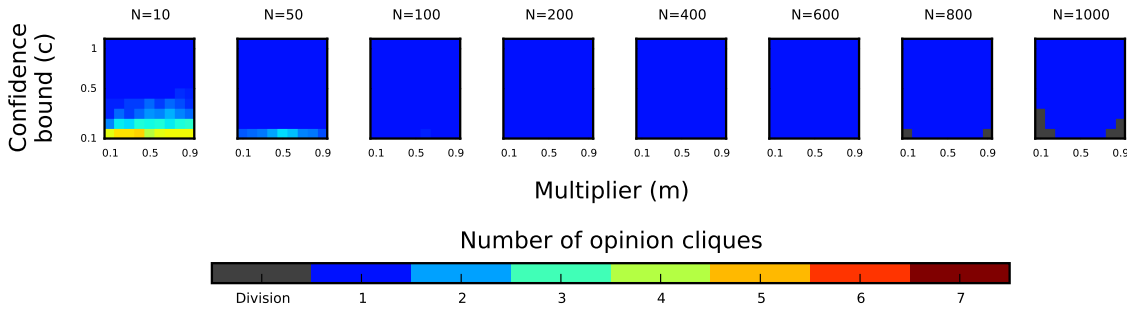

Figure 4.11: Summary of the number of opinion cliques that emerged in simulations on cycles for $N = 10, 50, 100, 200, 400, 600, 800,$ and 1000. These are representative of the trends that we observe in all simulations. We use grey colour to represent simulations that did not converge by the bailout time (10^9 time steps).

As shown in Figure 4.11, a consensus is reached for all simulations on cycles with $N = 100, 200, 400,$ and 600. Even though some simulations for $N = 1000$ did not converge by the bailout time, we conjecture that all simulations on cycles with large values of N will converge, independent of the values of c and m, if the Deffuant game is played for sufficiently many iterations. For N being 10 and 50, consensus is reached when $c \geq 0.5$. This observation is reasonable as, with fewer players connected on a circular network, their initial opinions are farther away from each other, which forces them to form more cliques. Similar to complete graphs, we observe that more opinion cliques tend to emerge in the final state as $m \to 0.5$ if multiple opinion cliques persist in the final state.

4.3   Annular lattices

In this section, we explore the behaviour of convergence time and the number of opinion cliques in the final state on annular lattices. We use simulation results on annular lattices

to compare with those on annular lattices with random edges.

Figure 4.12 summarises the values of $\ln(T)$ observed in simulations on annular lattices for which $N = 10, 50, 100, 200, 400, 600, 800,$ and 1000. Similar to complete graphs in Section 4.1, scatter plots of $\ln(T)$ against N, c, and m, show qualitatively distinct behaviour for $c < 0.5$ and $c \geq 0.5$. Thus, we conduct regression analysis for $c < 0.5$ and $c \geq 0.5$ separately.
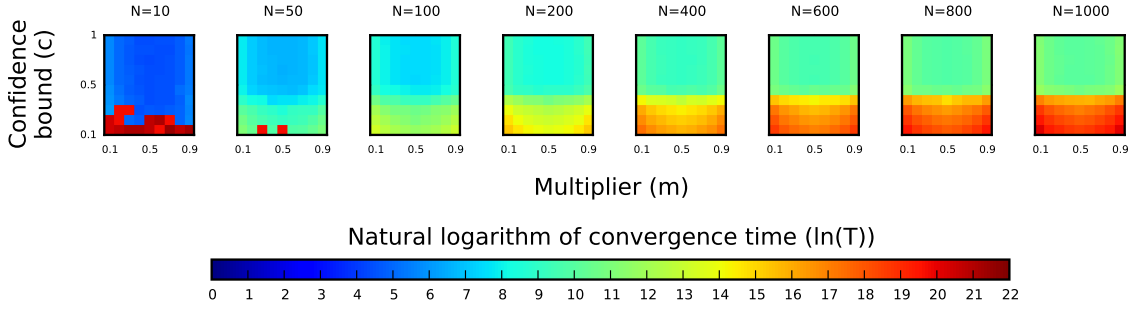

Figure 4.12: Summary of convergence time recorded in simulations on annular lattices for $N = 10, 50, 100, 200, 400, 600, 800,$ and 1000. These are representative of the trends that we observe in all simulations.

4.3.1 Convergence time

The case of $c < 0.5$

Following a similar AIC-based regression selection process as in Section 4.1, we arrive at the model

$$\ln(T)^2 = \beta_0 + \beta_1 N + \beta_2 N^2 + \beta_3 c + \beta_4 c^2 + \beta_5 (m - 0.5)^2 + \beta_6 Nc + \varepsilon. \tag{4.10}$$

Table 4.6 summarises the estimates for coefficients β_j ($j = 0, 1, \cdots, 6$) of Equation (4.10), accurate to 4 significant figures using scientific notation. For Equation (4.10), $R^2 \approx 0.9919$ and AIC ≈ 1301.9.

	Estimate	Std. Error	t value	$\Pr(> |t|)$
β_0	1.062×10^2	2.803	3.789×10	$< 2 \times 10^{-16}$
β_1	4.319×10^{-1}	$6.206 \times 10-3$	6.960×10	$< 2 \times 10^{-16}$
β_2	-1.790×10^{-4}	$4.822 \times 10-6$	-3.712×10	$< 2 \times 10^{-16}$
β_3	7.759×10	1.830×10	4.239	2.890×10^{-5}
β_4	-5.946×10^2	3.400×10	-1.749×10	$< 2 \times 10^{-16}$
β_5	2.839×10^2	5.924	4.792×10	$< 2 \times 10^{-16}$
β_6	-1.332×10^{-1}	$1.083 \times 10-2$	-1.230×10	$< 2 \times 10^{-16}$

Table 4.6: Summary of regression parameters for Equation (4.10), accurate to 4 significant figures using scientific notation.

The case of $c \geq 0.5$

Following a similar AIC-based regression selection process as in Section 4.1, we arrive at the model

$$\sqrt{\ln(T)} = \beta_0 + \beta_1 \ln(N) + \beta_2 c + \beta_3 c^2 + \beta_4 (m - 0.5)^2 + \beta_5 Nc + \varepsilon. \qquad (4.11)$$

Table 4.7 summarises the estimates for coefficients β_j ($j = 0, 1, \cdots, 5$) of Equation (4.11), accurate to 4 significant figures using scientific notation. For Equation (4.11), $R^2 \approx 0.9845$ and AIC ≈ -4219.1.

	Estimate	Std. Error	t value	$\Pr(> |t|)$
β_0	2.263	2.634×10^{-2}	8.592×10	$< 2 \times 10^{-16}$
β_1	2.072×10^{-1}	3.160×10^{-3}	6.556×10	$< 2 \times 10^{-16}$
β_2	-1.212	4.976×10^{-2}	-2.436×10	$< 2 \times 10^{-16}$
β_3	7.507×10^{-1}	3.273×10^{-2}	2.294×10	$< 2 \times 10^{-16}$
β_4	1.064	1.395×10^{-2}	7.624×10	$< 2 \times 10^{-16}$
β_5	-6.056×10^{-5}	9.865×10^{-6}	-6.138	1.650×10^{-9}

Table 4.7: Summary of regression parameters for Equation (4.11), accurate to 4 significant figures using scientific notation.

Summary of convergence time results

Through regression analysis, we obtained the models given by Equations (4.10) and (4.11) for annular lattices with confidence bounds $c < 0.5$ and $c \geq 0.5$ respectively. Similar to complete graphs, the different forms of these equations confirm our conjecture based on data exploration that convergence time, T, undergoes a transition for confidence bound being $c = 0.5$. As we stated in Section 4.1, one should conduct numerical simulations using $c \in (0.4, 0.5)$ in order to determine an accurate critical value for c.

Similar to complete graphs, T increases with the number of participating players, N. However, the effects of N, c, and m on T are coupled for annular lattices. In addition, T increases more rapidly for $c < 0.5$ than $c \geq 0.5$. With fixed values of N and c, T is symmetrical about multiplier being $m = 0.5$, at which value T obtains a minimum.

4.3.2 The number of opinion cliques

Figure 4.13 summarises the number of opinion cliques that persisted in the simulations on annular lattices for which the number of participating players are $N = 10, 50, 100, 200, 400, 600, 800,$ and 1000. A consensus is reached for all simulations on annular lattices with confidence bound being $c \geq 0.5$. For $N \geq 100$, the final state is mostly in polarisation at 2 distinct opinions when $c < 0.5$. For N being 10 and 50, multiple, sometimes more than 2, opinion cliques emerged in the final state. For a similar reason to that for cycles in Subsection 4.2.2, players' initial opinions are farther away from each other, as the number of players connected on an annular lattice decreases, which forces them to form more opinion cliques.
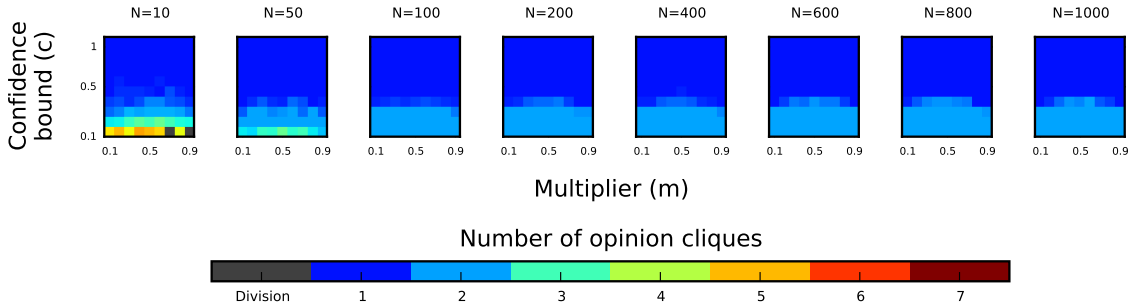
Figure 4.13: Summary of the number of opinion cliques that emerged in simulations on annular lattices for $N = 10, 50, 100, 200, 400, 600, 800$, and 1000. These are representative of the trends that we observe in all simulations. We use grey colour to represent simulations that did not converge by the bailout time (10^9 time steps).

4.4 Cycles with extra random edges

In this section, we explore the behaviour of convergence time and the number of opinion cliques in the final state on cycles with randomly generated extra edges. For a cycle with N nodes, we pick a pair of non-adjacent nodes uniformly at random and add an edge between them. We repeat this process sN times in order to add sN distinct extra edges to the cycle. We consider three values of s, namely 0.1, 0.2, and 0.3. Cycles with random edges are a version of the Watts-Strogatz model with original connectivity 2. The Watts-Strogatz model captures two properties that are commonly observed in real social networks, which are high clustering, meaning that individuals with mutual friends tend to be friends as well, and short average path lengths [52].

4.4.1 Convergence time

Figure 4.14 summarises the values of $\ln(T)$ observed in simulations on cycles with randomly generated extra edges for which the number of participating players are $N = 10, 50, 100, 200, 400, 600, 800$, and 1000.

Following a similar AIC-based regression selection process as in Section 4.1, we arrive at the model

$$\ln(T)^{\alpha} = \beta_0 + \beta_1 \ln(N) + \beta_2 N + \beta_3 N^2 + \beta_4 c + \beta_5 c^2 + \beta_6 (m - 0.5)^2 + \beta_7 Nc + \varepsilon, \quad (4.12)$$

where the power transformation parameter α is given by $\alpha = -\frac{1}{3}, -\frac{2}{3}$, and $-\frac{5}{6}$ for $s = 0.1$, 0.2, and 0.3, respectively. For $s = 0.1$, the Nc term is statistically insignificant and thus is dropped during model reduction. Table 4.8 summarises the estimates for coefficients β_j ($j = 0, 1, \cdots, 7$) of Equation (4.12), accurate to 4 significant figures using scientific notation.

As we have observed in all the networks considered so far, convergence time, T, increases with the number of participating players, N. However, regression analysis suggests no transition of T with respect to confidence bound, c. Instead, T increases more rapidly
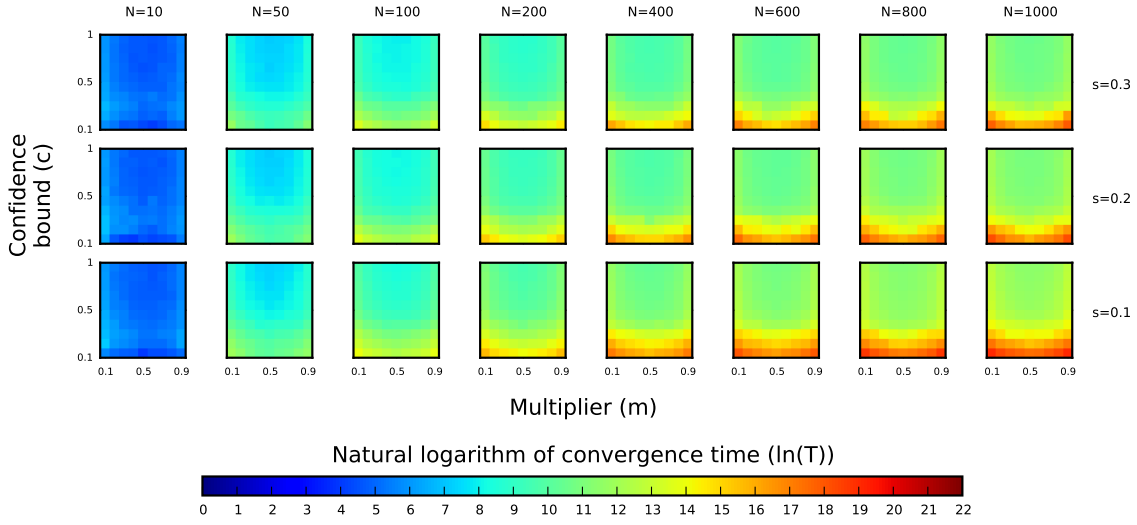
Figure 4.14: Summary of convergence time recorded in simulations on cycles with sN extra randomly generated edges for $N = 10$, 50, 100, 200, 400, 600, 800, and 1000. These are representative of the trends that we observe in all simulations.

s	β_0	β_1	β_2	β_3	β_4	β_5	β_6	β_7
0.1	5.485×10^{-1}	-3.140×10^{-2}	6.760×10^{-5}	-2.908×10^{-8}	1.820×10^{-1}	-1.101×10^{-1}	-9.576×10^{-2}	N/A
0.2	2.763×10^{-1}	-2.351×10^{-2}	4.343×10^{-5}	-1.653×10^{-8}	1.779×10^{-1}	-1.084×10^{-1}	-8.901×10^{-2}	-1.008×10^{-5}
0.3	2.031×10^{-1}	-1.977×10^{-2}	3.548×10^{-5}	-1.090×10^{-8}	1.452×10^{-1}	-8.829×10^{-2}	-7.934×10^{-2}	-1.093×10^{-5}

Table 4.8: Estimates for the coefficients of Equation (4.12) for cycles with sN extra random edges, where N is the number of players in the network. Estimates are accurate to 4 significant figures using scientific notation. For $s = 0.1$, the Nc term is statistically insignificant and thus is dropped during model reduction, which corresponds to the entry $\beta_7 = $ N/A in the table. For $s = 0.1$, AIC ≈ -10378.2 and $R \approx 0.9853$. For $s = 0.2$, AIC ≈ -10443.3 and $R \approx 0.9829$. For $s = 0.3$, AIC ≈ -10719.2 and $R \approx 0.9816$.

with N for $c < 0.5$ than $c \geq 0.5$. Adding extra random edges to cycles decreases convergence time significantly. In addtion, T increases much more slowly with N on cycles with random edges than on cycles. Interestingly, the weak coupling term Nm becomes less statistically significant and finally changes to the weak coupling term Nc, as we add more random edges to a cycle. We also note that T is roughly symmetric about the multiplier value of $m = 0.5$, with the smallest values of T occuring around $m = 0.5$.

4.4.2   The number of opinion cliques

Figure 4.15 summarises the number of opinion cliques that emerged in simulations on cycles with randomly generated extra edges for which $N = 10$, 50, 100, 200, 400, 600, 800, and 1000. For a small proportion of random edges, the number of opinion cliques in the final state is roughly the same as observed in simulations on cycles. However, multiple opinion cliques emerge in the final state for $c \geq 0.3$ and $N \geq 100$. We conjecture that the number of opinion cliques in the final state, K, behaves more like in the case of complete

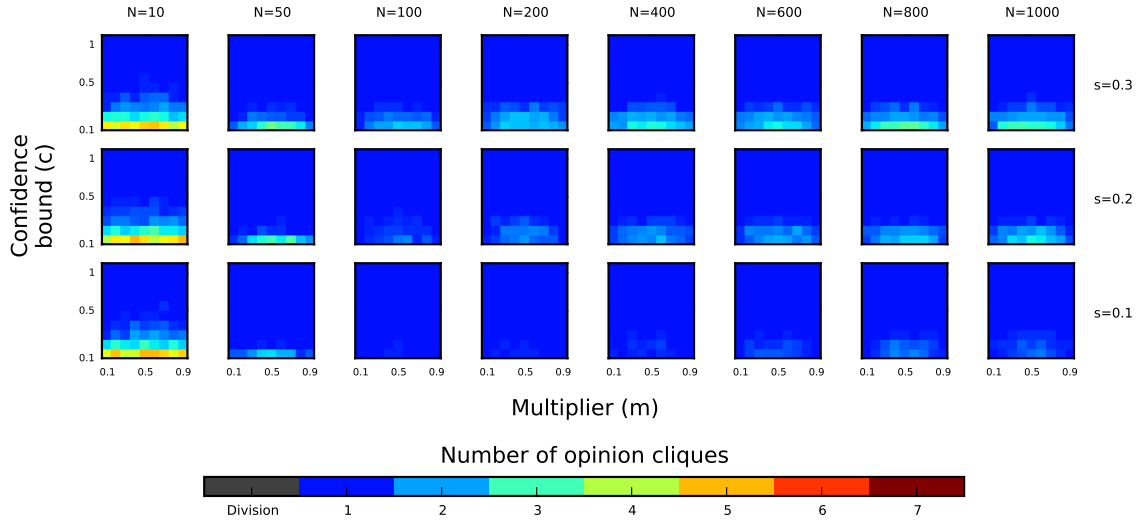graphs as more random edges are added with respect to the value of N.

Figure 4.15: Summary of the number of opinion cliques that emerged in simulations on cycles with random edges for $N = 10$, 50, 100, 200, 400, 600, 800, and 1000. These are representative of the trends that we observe in all simulations. We use grey colour to represent simulations that did not converge by the bailout time (10^9 time steps).

4.5 Annular lattices with extra random edges

In this section, we explore the behaviour of convergence time and the number of opinion cliques in the final state on annular lattices with random edges that are generated using the same mechanism as in Section 4.4. We also consider $s = 0.1$, 0.2, and 0.3. Annular lattices with random edges are a version of the Watts-Strogatz model with original connectivity 3.

Figure 4.16 summarises the values of $\ln(T)$ observed in simulations on annular lattices with randomly generated extra edges for the cases $N = 10$, 50, 100, 200, 400, 600, 800, and 1000. Similar to annular lattices in Section 4.3, we observe qualitatively distinct behaviour of convergence time for $c < 0.5$ and $c \geq 0.5$ on annular lattices with extra randomly generated random edges. Thus, we conduct regression analysis for these two cases separately.

4.5.1 Convergence time

The case of $c < 0.5$

Following a similar AIC-based regression selection process as in Section 4.1, we arrive at the model

$$\ln(T) = \beta_0 + \beta_1 N + \beta_2 N^2 + \beta_3 c + \beta_4 c^2 + \beta_5 (m - 0.5)^2 + \beta_6 Nc + \varepsilon. \tag{4.13}$$

Table 4.9 summarises the estimates for coefficients β_j ($j = 0, 1, \cdots, 6$) of Equation (4.13), accurate to 4 significant figures using scientific notation.
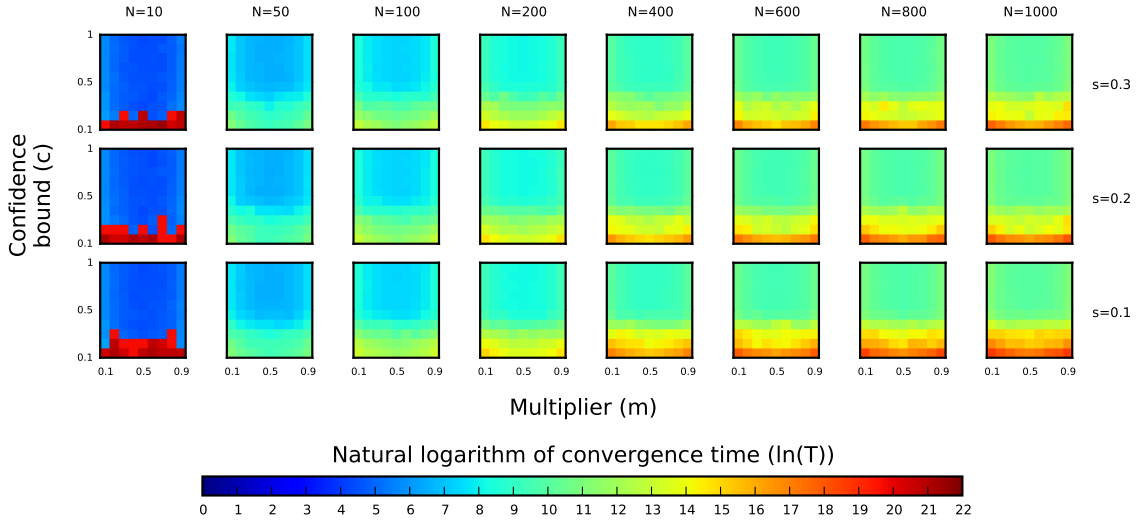
Figure 4.16: Summary of convergence time recorded in simulations on annular lattices with extra randomly generated edges for $N = 10, 50, 100, 200, 400, 600, 800$, and 1000. These are representative of the trends that we observe in all simulations.

s	β_0	β_1	β_2	β_3	β_4	β_5	β_6
0.1	1.225×10	1.240×10^{-2}	-6.048×10^{-6}	-6.132	-1.078×10	6.183	-5.739×10^{-3}
0.2	1.309×10	1.067×10^{-2}	-5.535×10^{-6}	-1.699×10	1.088×10	6.064	-4.199×10^{-3}
0.3	1.353×10	8.670×10^{-3}	-4.073×10^{-6}	-2.060×10	1.764×10	6.879	-3.324×10^{-3}

Table 4.9: Estimates for the coefficients of Equation (4.13) and the corresponding coefficients of determination for annular lattices with sN extra random edges, where N is the number of players in the network. Estimates are accurate to 4 significant figures using scientific notation. For $s = 0.1$, AIC ≈ -592.1 and $R \approx 0.9613$. For $s = 0.2$, AIC ≈ -427.99 and $R \approx 0.9283$. For $s = 0.3$, AIC ≈ -482.58 and $R \approx 0.9336$.

The case of $c \geq 0.5$

Following a similar AIC-based regression selection process as in Section 4.1, we arrive at the model

$$\ln(T) = \beta_0 + \beta_1 \ln(N) + \beta_2 c + \beta_3 c^2 + \beta_4 (m - 0.5)^2 + \beta_5 Nc + \varepsilon. \qquad (4.14)$$

Table 4.10 summarises the estimates for coefficients β_j ($j = 0, 1, \cdots, 5$) of Equation (4.14), accurate to 4 significant figures using scientific notation.

Summary of convergence time results

Through regression analysis, we obtained the models given by Equations (4.13) and (4.14) for annular lattices with random edges for confidence bounds $c < 0.5$ and $c \geq 0.5$ respectively. The different forms of these equations confirm our conjecture based on data exploration that convergence time, T, undergoes a transition at $c = 0.5$. Again, one should

s	β_0	β_1	β_2	β_3	β_4	β_5
0.1	3.528	1.200	−4.263	2.628	6.720	-2.061×10^{-4}
0.2	3.300	1.161	−3.242	2.002	6.634	-1.808×10^{-4}
0.3	3.193	1.116	−2.436	1.465	6.671	-5.580×10^{-5}

Table 4.10: Estimates for the coefficients of Equation (4.13) and the corresponding coefficients of determination for annular lattices with sN extra random edges, where N is the number of players in the network. The estimates are accurate to 4 significant figures using scientific notation. For $s = 0.1$, AIC ≈ 2596.67 and $R \approx 0.9914$. For $s = 0.2$, AIC ≈ -2693.1 and $R \approx 0.9922$. For $s = 0.3$, AIC ≈ -2912.41 and $R \approx 0.9947$.

conduct numerical simulations using $c \in (0.4, 0.5)$ in order to determine an accurate critical value for c. Regression analysis suggests that adding random edges to annular lattices decreases T more for $c < 0.5$ than it does for $c \geq 0.5$.

4.5.2 The number of opinion cliques

Figure 4.17 summarises the number of opinion cliques that emerged in simulations on annular lattices with randomly generated extra edges for which $N = 10, 50, 100, 200, 400, 600, 800,$ and 1000.
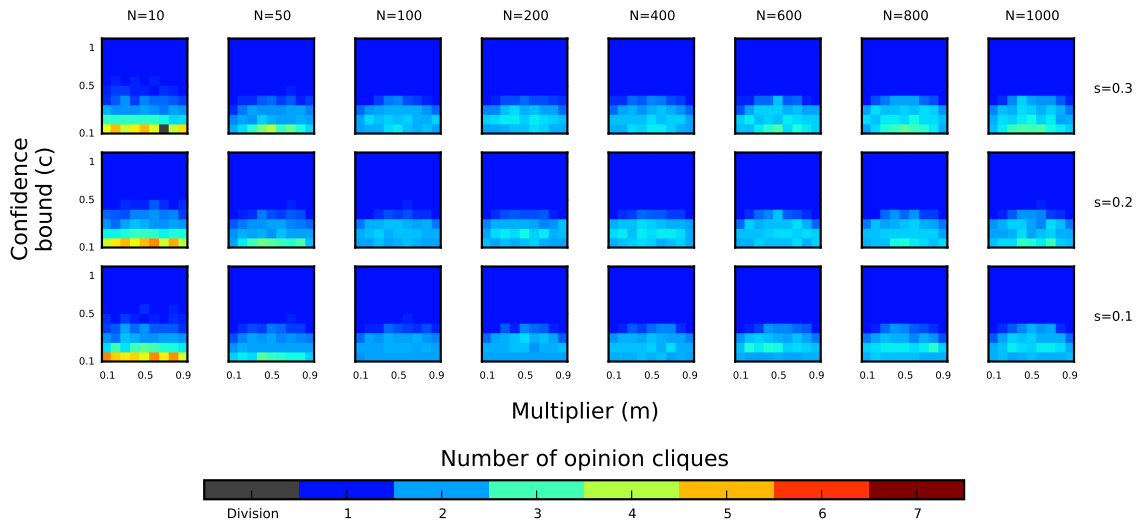

Figure 4.17: Summary of the number of opinion cliques that emerged in simulations on annular lattices with random edges for $N = 10, 50, 100, 200, 400, 600, 800,$ and 1000. These are representative of the trends that we observe in all simulations. We use grey colour to represent simulations that did not converge by the bailout time (10^9 time steps).

As was true for annular lattices, censensus is always reached on annular lattices with random edges for confidence bound being $c \geq 0.5$. For $c < 0.5$, however, $K \approx 3$ when $N \geq 50$, in contrast with $K \approx 2$ for annular lattices.

4.6 Erdős-Rényi model

In this section, we explore the behaviour of convergence time and the number of opinion cliques in the final state on random graphs generated by the Erdős-Rényi $G(N,p)$ model, where p is the independent probability to add an edge between a pair of nodes. The Erdős-Rényi model is one of the best studied models of network and has been used to study the Deffuant model in some literature [5, 24, 40, 41]. However, existing research of the Deffuant model on Erdős-Rényi random graphs has mainly focused on adaptive networks that evolve with the game [40, 41]. We consider the Erdős-Rényi $G(N,p)$ model for $p = 0.1, 0.2, \cdots, 0.9$. Complete graphs are a special case of the Erdős-Rényi $G(N,p)$ model with $p = 1$.

Figure 4.18 presents a subset of the values of $\ln(T)$ recorded in simulations, which are representative of the observed trends in all simulations. The scatter plots of T against N, c, and m are similar to those of complete graphs (Figure 4.2), which also show qualitatively distinct behaviour for $c < 0.5$ and $c \geq 0.5$.
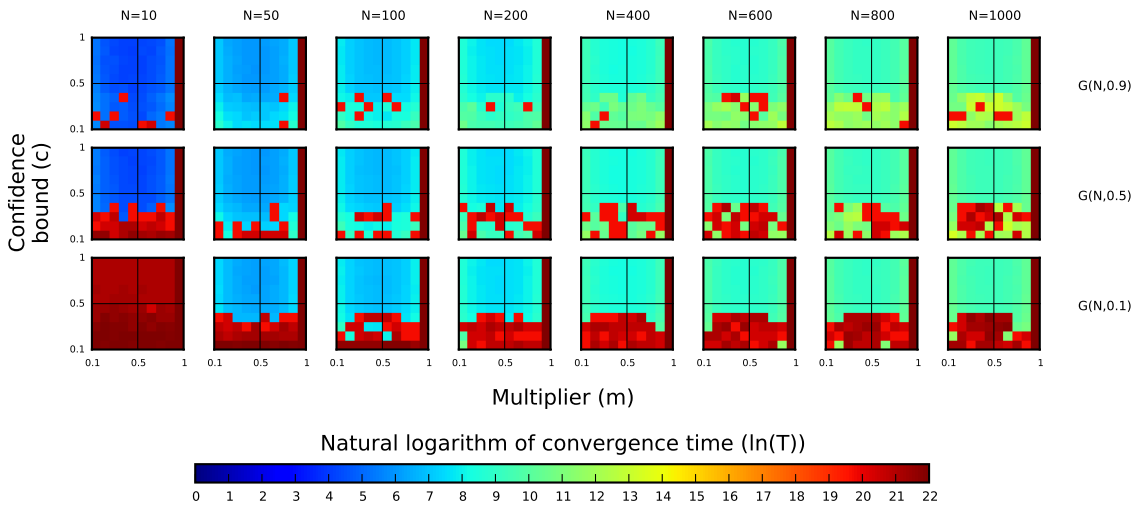

Figure 4.18: Summary of simulations on random graphs generated by the Erdős-Rényi $G(N,p)$ model. We conducted simulations for $p = 0.1, 0.2, \cdots, 0.9$, and present a subset of the plots here which are sufficient to show the observed trends.

4.6.1 Convergence time

The case of $c < 0.5$

Following a similar AIC-based regression selection process as in Section 4.1, we arrive at the model

$$\ln(\ln(T)) = \beta_0 + \beta_1 N + \beta_2 N^2 + \beta_3 c^2 + \beta_4 (m - 0.5)^2 + \beta_5 Nc + \varepsilon. \qquad (4.15)$$

Random graphs generated by the Erdős-Rényi $G(N,p)$ model adds more stochasticity to the game, which accounts for the increased number of outliers observed in the simulation

results as compared with simulations on complete graphs. For each value of p, Table 4.11 summarises estimates for the coefficients of Equation (4.15). In the caption of Table 4.11, we also give the proportion ($q \in [0, 1]$) of data points that we identify as extreme outliers and exclude from our regression analysis. We only consider the $G(N, p)$ models for $p = 0.7$, 0.8, and 0.9, as $q > 0.15$ for smaller values of p, which can undermine the reliability of the regression analysis.

p	β_0	β_1	β_2	β_3	β_4	β_5
0.7	2.098	8.744×10^{-4}	-4.854×10^{-7}	-8.606×10^{-1}	2.294×10^{-1}	N/A
0.8	2.111	8.328×10^{-4}	-4.349×10^{-7}	-7.874×10^{-1}	1.255×10^{-1}	N/A
0.9	2.117	7.901×10^{-4}	-4.327×10^{-7}	-8.926×10^{-1}	1.200×10^{-1}	2.323×10^{-4}

Table 4.11: Estimates for the coefficients of Equation (4.15) for the Erdős-Rényi $G(N, p)$ model with $c < 0.5$, accurate to 4 significant figures using scientific notation. For $p = 0.7$, $q \approx 0.1133$, AIC ≈ -1515.5, and $R \approx 0.8360$. For $p = 0.8$, $q \approx 0.0767$, AIC ≈ -1658.1, and $R \approx 0.8114$. For $p = 0.9$, $q = 0.05$, AIC ≈ -1774.1, and $R \approx 0.7984$.

The case of $c \geq 0.5$

Following a similar AIC-based regression selection process as in Section 4.1, we arrive at the model given by Equation (4.8) for all the values of p considered. For each value of p, Table 4.12 summarises estimates for the coefficients β_j ($j = 0, 1, \cdots, 3$) of Equation (4.8), together with the corresponding values of AIC and R^2.

p	β_0	β_1	β_2	β_3	AIC	R^2
0.1	1.953	1.050	4.412×10^{-1}	6.362	-3156.1	0.9958
0.2	1.931	1.053	4.500×10^{-1}	6.290	-3194.2	0.9961
0.3	1.918	1.055	4.512×10^{-1}	6.275	-3215.1	0.9962
0.4	1.886	1.060	4.453×10^{-1}	6.270	-3233.7	0.9963
0.5	1.827	1.068	4.548×10^{-1}	6.284	-3209.2	0.9963
0.6	1.870	1.062	4.499×10^{-1}	6.255	-3233.6	0.9964
0.7	1.851	1.065	4.470×10^{-1}	6.242	-3213.7	0.9963
0.8	1.873	1.061	4.555×10^{-1}	6.289	-3267.4	0.9966
0.9	1.838	1.067	4.676×10^{-1}	6.261	-3251.8	0.9965
1	1.865	1.062	4.530×10^{-1}	6.262	-3240.9	0.9964

Table 4.12: Estimates for the coefficients of Equation (4.8) and the corresponding values of R^2 and AIC for the Erdős-Rényi $G(N, p)$ model for which $c \geq 0.5$, accurate to 4 and 5 significant figures using scientific notation respectively. For comparison, we also include the coeffcients of the model for complete graphs studied in Section 4.1.

Summary of convergence time results

Through regression analysis, we obtained the models given by Equations (4.15) and (4.8) for the Erdős-Rényi $G(N,p)$ model for confidence bounds being $c < 0.5$ and $c \geq 0.5$ respectively. The different forms of these equations confirm our conjecture based on data exploration that convergence time, T, undergoes a transition at $c = 0.5$. Again, one should conduct numerical simulations using $c \in (0.4, 0.5)$ in order to determine an accurate critical value for c.

For $c < 0.5$, multiplier m affects T through the $(m - 0.5)^2$ term. In contrast, the regression model for complete graphs (Equation (4.5)) suggests independence of T on m. For the Erdős-Rényi $G(N,p)$ model, the effect of m on T is independent of N and c. In addition, T is symmetrical about $m = 0.5$, obtaining a minimum at $m = 0.5$ if N and c are fixed.

For $c \geq 0.5$, the regression model is Equation (4.8), which is the same as that for complete graphs. We do not observe a clear trend of the estimated coefficients β_j ($j = 0, 1, 2, 3$) with respect to p. For large values of p, the estimated coefficients are very close to those for complete graphs. This suggests that one can probably use a mean-field approximation to study convergence time on the Erdős-Rényi $G(N,p)$ model if p is close to 1.

4.6.2 The number of opinion cliques

Figure 4.19 summarises the number of opinion cliques that emerged in simulations on random graphs generated by the Erdős-Rényi $G(N,p)$ model for which $N = 10, 50, 100, 200, 400, 600, 800,$ and 1000.

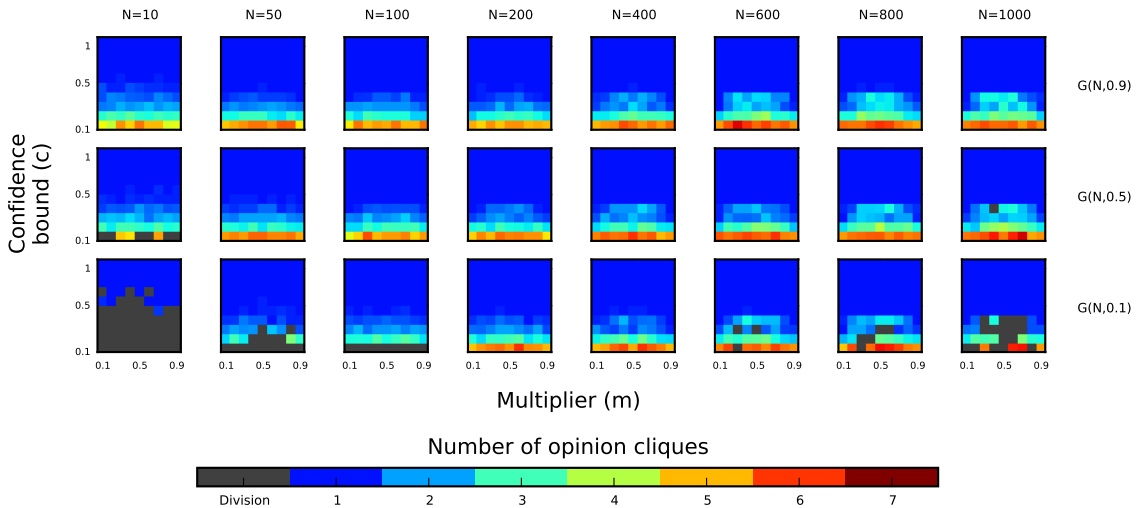
Figure 4.19: Summary of the number of opinion cliques that emerged in simulations on Erdős-Rényi $G(N,p)$ models. We conducted simulations for $p = 0.1, 0.2, \cdots, 0.9$, and present a subset of the plots here which are sufficient to show the observed trends. We use grey colour to represent simulations that did not converge by the bailout time (10^9 time steps).

For values of edge probability, p, close to 1, the behaviour of the number of opinion

cliques in the final state, K, is similar to what is observed on complete graphs. As $p \to 0$, the major difference is that opinions will fail to converge within the bailout time for small values of confidence bound, c.

5 Discussions

The Deffuant model is an example of a discrete-time repeated game, played pair-wise among a group of players that are connected via a network. At each time step, randomly selected neighbouring players interact pairwise and make a compromise toward each others opinion whenever their opinion difference is less than a given threshold. The game is played until the players' opinions converge. There are four ways through which one can manipulate the game, namely the structure of the network on which players are connected, the number of players that participate in the game (N), the population's confidence bound (c), and their openness of mind (m). In this report, we have investigated the Deffuant model on various networks in a systematic manner. In particular, we have modelled the convergence time of opinions, T, as a function of N, c, and m through numerical simulations and linear regression analysis for each network topology considered. We have also studied the number of opinion cliques in the final state, K, qualitatively, as such approach is more natural than conducting regression analysis due to the more complicated nature of the opinion clique distributions.

We have studied two types of networks, one having deterministic structures and the other being generated randomly according to some stochastic rules. The deterministic networks studied consist of complete graphs, cycles, and annular lattices, all of which are regular graphs. These networks provide simulation results for us to compare with those on random graphs. In addition, complete graphs can be used to model small communities, where everyone knows each other, and as approximations to communities in large social networks [51]. The random graphs considered consist of cycles and annular lattices with randomly generated extra edges, and random graphs generated by the Erdős-Rényi $G(N, p)$ model. These graphs possess some properties that social networks often exhibit. For example, cycles and annular lattices with random edges are a version of the Watts-Strogatz model and capture the properties of high clustering and short average path lengths, which are commonly observed in real social networks [52]. Meanwhile, the Erdős-Rényi model is one of the best studied models of network science and has been used to study the Deffuant model in some literature [5, 24, 40, 41, 52].

We first summarise the convergence time results. For the collection of networks with deterministic structures, the Deffuant model converges fastest on complete graphs and slowest on cycles. This observation suggests that the convergence time of opinions, T, decreases with an increase in the density of edges in a network. Interestingly, regression analysis reveals that T undergoes a transition at a value of the confidence bound equal to $c = 0.5$ on complete graphs and annular lattices, while such a transition is not seen on cycles. When such a transition occurs, T is much smaller for $c \geq 0.5$ than for $c < 0.5$. Another notable phenomenon is that the interplay among the effects of N, c, and m on T is different when the underlying interaction network changes. For example, the effects of the three parameters on T are independent on complete graphs with $c \geq 0.5$, whereas N and m are weakly coupled for cycles, and all of the three parameters are coupled for annular

lattices. A common trait that we have found on all of these three deterministic networks is that T increases with N.

For the random graph models considered, whether there exists a transition in the behaviour of T with respect to c is consistent with their deterministic counterpart networks. Recall that complete graphs can be interpreted as graphs generated by a special case of the Erdős-Rényi $G(N, p)$ model with $p = 1$. Regression analysis suggests that adding random edges to cycles and annular lattices decreases T dramatically. For annular lattices, the decrease in T due to the addition of random edges is sharper for $c < 0.5$ than for $c \geq 0.5$. In addition, T increases much more slowly with N on cycles with random edges than it does on cycles. The same observation holds for annular lattices and their random graph counterparts in the region $c < 0.5$. For the Erdős-Rényi $G(N, p)$ model, the regression model is very similar to that of complete graphs for large values of the edge generation probability, p. This suggests that one can probably use a mean-field approximation to study convergence time on the Erdős-Rényi model if p is close to 1. Overall, our regression analysis also indicates that T is symmetric about $m = 0.5$ on complete graphs when $c \geq 0.5$, on annular lattices with random edges for all $c \in [0, 1]$, and on random graphs generated by the Erdős-Rényi model when $c \geq 0.5$.

In terms of the number of opinion cliques in the final state, K, consensus is reached for $c \geq 0.5$ on all three of the deterministic networks, whereas more opinion cliques persist as the node degree of a regular graph increases for $c < 0.5$. A possible reason for this phenomenon is that players who are connected on a regular graph with a higher node degree have more neighbours with 'competing' opinions, which gives the players less time to make up their minds, and thus more opinion cliques persist. Adding a small proportion of random edges to cycles in terms of N does not have a large impact on the number of opinion cliques in the final state. However, multiple opinion cliques emerge in the final state for $c \geq 0.2$ and $N \geq 100$, whereas consensus is reached on cycles for $N \geq 100$ except for 9 out of 540 combinations of N, c, and m. For the cases that did not converge by the bailout time, it is possible that the opinions will converge to censensus if the Deffuant game is played for sufficiently many iterations. We conjecture that K behaves more like in the case of complete graphs as we add more random edges to cycles with respect to the value of N. In contrast, adding more random edges to annular lattices makes the final state changes from polarisation at $K = 2$ different opinions to fragmentation where there are $K > 2$ opinion cliques. For the Erdős-Rényi $G(N, p)$ model, the behaviour of K is similar to what is observed on complete graphs when the edge generation probability, p, is close to 1. As the value of p decreases, we observe that convergence fails to occur before the bailout time, for small enough values of c.

Our results provide insight into how some real-world happenings can be steered towards desired outcomes as well as implications for the study of voting games. For instance, when a convention wants to reach a censensus, it is often desirable to let attendants agree in shortest time that is possible. In such a scenario, the meeting's organisers should encourage people to embrace diverse opinions. Introducing strangers so that they have conversations may speed up the process for attendants to make up their minds, but this may lead the crowds to divide into groups with opposing viewpoints. While planning such a meeting, the organiser should be aware that the more people there are invited, the longer it will likely

to take for the attendants to narrow down their opinions to a few options for voting. In some other cases, such as campaigns to prevent certain wrong beliefs to spread, the government should caution people against trusting bizarre opionions and suggest that people agree with others who share similar viewpoints instead.

There are several possible extensions to the work in this report. First, we have considered three deterministic networks and three random graph models, and it will be valuable to study the Deffuant model on more network structures. In particular, it would be interesting to conduct numerical simulations on random networks that are generated using some properties of real social networks, such as friendships on Facebook. Second, opinions in some of our simulations did not converge by the bailout time, and we averaged convergence time and the number of opinion cliques in the final state over 10 groups of independent simulations for each network and each combination of N, c, and m, considered in order to smooth out noise caused by the stochasticity of the initial opinion profiles and the order of players' pairwise interaction. Having more than 10 groups in each simulation and longer bailout time would generate data points that are more accurate for regression analysis. In addition, studying generalisations of the Deffuant model on various networks in a systematic manner, as we did here for the standard Deffuant model could provide more accurate insight into real-world applications.

Bibliography

[1] Acemoglu, D., Como, G., Fagnani, F., and Ozdaglar, A., Opinion fluctuations and disagreement in social networks, *Math. Oper. Res.*, **38**(1), 1–27 (2013).

[2] Acemoglu, D., Dahleh, M. A., Lobel, I., and Ozdaglar, A., Bayesian learning in social networks, *Rev. Econ. Stud.*, **78**(4), 1201–1236 (2011).

[3] Acemoglu, D. and Ozdaglar, A., Opinion dynamics and learning in social networks, *Dyn. Games Appl.*, **1**(1), 3–49 (2011).

[4] Akaike, H., A new look at the statistical model identification, *IEEE Trans. Autom. Control*, **19**(6), 716–723 (1973).

[5] Alaai, A., Purvis, M. A., and Savarimuthu, B. T. R., Vector opinion dynamics: An extended model for consensus in social networks, in *Proceedings of the 2008 IEEE/WIC/ACM International Conference on Web Intelligence and Intelligent Agent Technology*, pp. 394–397, IEEE Computer Society, Washington, DC (2008).

[6] Amblard, F. and Deffuant, G., The role of network topology on extremism propagation with relative agreement opinion dynamics, *Physica A*, **343**, 725–738 (2004).

[7] Barabási, A.-L. and Albert, R., Emergence of scaling in random networks, *Science*, **286**(5439), 509–512 (1999).

[8] Barabási, A.-L., Gulbahce, N., and Loscalzo, J., Network medicine: A network-based approach to human disease, *Nat. Rev. Genet.*, **12**(1), 56–68 (2011).

[9] Barrat, A., Barthélemy, M., and Vespignani, A., *Dynamical processes on complex networks*, Cambridge University Press, Cambridge (2008).

[10] Ben-Naim, E., Krapivsky, P. L., and Redner, S., Bifurcations and patterns in compromise processes, *Physica D*, **183**(3–4), 190–204 (2003).

[11] Boccaletti, S., Latora, V., Moreno, Y., Chavez, M., and Hwang, D.-U., Complex networks: Structure and dynamics, *Phys. Reps.*, **424**(4–5), 175–308 (2006).

[12] Box, G. E. P. and Cox, D. R., An analysis of transformations, *J. R. Stat. Soc. Ser. B*, **26**, 211–234 (1964).

[13] Castellano, C., Fortunato, S., and Loreto, V., Statistical physics of social dynamics, *Rev. Mod. Phys.*, **81**(2), 591–646 (2009).

[14] Chamley, C., Scaglione, A., and Li, L., Models for the diffusion of beliefs in social networks: An overview, *IEEE Signal Process. Mag.*, **30**(3), 16–29 (2013).

[15] Clifford, P. and Sudbury, A., A model for spatial conflict, *Biometrika*, **60**(3), 581–588 (1973).

[16] Cohen, R. and Havlin, S., *Complex networks: Structure, robustness and function*, Cambridge University Press, Cambridge (2010).

[17] Cook, R. D., Detection of influential observation in linear regression, *Technometrics*, **19**(1), 15–18 (1977).

[18] Deffuant, G., Neau, D., Amblard, F., and Weisbuch, G., Mixing beliefs among interacting agents, *Adv. Complex Syst.*, **3**(1), 87–98 (2000).

[19] Deffuant, G., Amblard, F., Weisbuch, G., and Faure, T., How can extremism prevail? A study based on the relative agreement interaction model, *J. Art. Soc. Soc. Simul.*, **5**(4) (2002).

[20] Deffuant, G., Amblard, F., and Weisbuch, G., Modelling group opinion shift to extreme: The smooth bounded confidence model, arXiv preprint cond-mat/0410199 (2004).

[21] Di Mare, A. and Latora, V., Opinion formation models based on game theory, *Int. J. Mod. Phys. C*, **18**(9), 1377–1395 (2007).

[22] Draper, N. R. and Smith, H., *Applied Regression Analysis*, John Wiley & Sons, New York, 2nd ed. (1981).

[23] Erdős, P. and Rényi, A., On random graphs, *Publ. Math. Debrecen*, **6**, 290–297 (1959).

[24] Fortunato, S., Universality of the threshold for complete consensus for the opinion dynamics of Deffuant *et al.*, *Int. J. Mod. Phys. C*, **15**(9), 1301–1307 (2004).

[25] Fortunato, S., Latora, V., Pluchino, A., and Rapisarda, A., Vector opinion dynamics in a bounded confidence consensus model, *Int. J. Mod. Phys. C*, **16**(10), 1535–1551 (2005).

[26] Freeman, D. A., *Statistical Models: Theory and Practice*, Cambridge University Press, Cambridge (2005).

[27] Fudenberg, D. and Tirole, J., *Game Theory*, MIT Press, Cambridge (1995).

[28] Galam, S., Minority opinion spreading in random geometry, *Eur. Phys. J. B*, **25**, 403–406 (2002).

[29] Gandica, Y., del Castillo-Mussot, M., Vázquez, G. J., Rojas, S., Continuous opinion model in small-world directed networks, *Physica A*, **389**(24), 5864–5870 (2010).

[30] Gilbert, E. N., Random graphs, *Ann. Math. Stat.*, **30**(4), 1141–1144 (1959).

[31] Hegselmann, R. and Krause, U., Opinion dynamics and bounded confidence: Models, analysis and simulation, *J. Artif. Soc. Soc. Simul.*, **5**(3), 1–24 (2002).

[32] Holley, R. A. and Liggett, T. M., Ergodic theorems for weakly interacting infinite systems and the voter model, *Ann. Probab.*, **3**(4), 643–663 (1975).

[33] Hunter, J. D., Matplotlib: A 2D graphics environment, *Comput. Sci. Eng.*, **9**(3), 90–95, http://matplotlib.org/ (2007).

[34] Iñiguez, G., Kertész, J., Kaski, K. K., and Barrio, R. A., Opinion and community formation in coevolving networks, *Phys. Rev. E*, **80**(6), 066119 (2009).

[35] Jackson, M. O., *Social and Economic Networks*, Princeton University Press, Princeton (2008).

[36] Jackson, M. O. and Zenou, Y., Games on networks, *Handbook of Game Theory*, **4** (2014).

[37] Focusing of opinions in the Deffuant model: First impression counts, *Int. J. Mod. Phys. C*, **17**(12), 1801–1808 (2006).

[38] Jalili, M., Social power and opinion formation in complex networks, *Physica A*, **392**(4), 959–966 (2013).

[39] Kivelä, M., Arenas, A., Barthelemy, M., Gleeson, J. P., Moreno, Y., and Porter, M. A., Multilayer networks, *J. Complex Netw.*, **2**(3), 203–271 (2014).

[40] Kozma, B. and Barrat, A., Consensus formation on adaptive networks, *Phys. Rev. E*, **77**(1), 016102 (2008).

[41] Kozma, B. and Barrat, A., Consensus formation on coevolving networks: groups' formation and structure, *J. Phys. A: Math. Theor.*, **41**(22), 224020 (2008).

[42] Krause, U., A discrete nonlinear and non-autonomous model of consensus formation, in S. Elaydi, G. Ladas, J. Popenda, and J. Rakowski, eds., *Communications in Difference Equations*, *Proceedings of the Fourth International Conference on Difference Equations*, pp. 227–236, CRC Press, Poznan (2000).

[43] Laguna, M. F., Abramson, G., and Zanette, D. H., Minorities in a model for opinion formation, *Complexity*, **9**(4), 31–36 (2004).

[44] Landau, D. P. and Binder, K., *A Guide to Monte Carlo Simulations in Statistical Physics*, Cambridge University Press, New York, 4th ed. (2014).

[45] Latané, B., The psychology of social impact, *Am. Psychol.*, **36**(4), 343–356 (1981).

[46] Lorenz, J., A stabilization theorem for dynamics of continuous opinions, *Physica A*, **355**(1), 217–223 (2005).

[47] Lorenz, J., Continuous opinion dynamics: Insights through interactive Markov chains, arXiv preprint 0708.3293 (2005).

[48] Lorenz, J., Continuous opinion dynamics under bounded confidence: A survey, *Int. J. Mod. Phys. C*, **18**(12), 1819–1838 (2007).

[49] Lorenz, J., Heterogeneous bounds of confidence: Meet, discuss and find consensus!, *Complexity*, **15**(4), 43–52 (2010).

[50] Lorenz, J. and Urbig, D., About the power to enforce and prevent consensus by manipulating communication rules, *Adv. Complex Syst.*, **10**(2), 251–269 (2007).

[51] Luce, R. D. and Perry, A. D., A method of matrix analysis of group structure, *Psychometrika*, **14**(2), 95–116 (1949).

[52] Newman, M. E. J., *Networks: An Introduction*, Oxford University Press, Oxford (2010).

[53] Newman, M. E. J. and Watts, D. J., Scaling and percolation in the small-world network model, *Phys. Rev. E*, **60**(6), 7332–7342 (1999).

[54] Nicholls, G., Lecture notes for Part B Applied Statistics, Department of Statistics, University of Oxford, version of 28 November 2014, http://www.stats.ox.ac.uk/~nicholls/sb1a/lectures5-6.pdf.

[55] Nowak, A., Szamrej, J., and Latané, B., From private attitude to public opinion: A dynamic theory of social impact, *Psychol. Rev.*, **97**(3), 362–376 (1990).

[56] Osborne, J. W., Improving your data transformations: Applying the Box-Cox transformation, *Practical Assessment, Research & Evaluation*, **15**(12), 1–9 (2010).

[57] Pluchino, A., Latora, V., and Rapisarda, A., Changing opinions in a changing world: A new perspective in sociophysics, *Int. J. Mod. Phys. C*, **16**(4), 515 (2005).

[58] Porfiri, M., Bollt, E. M., and Stilwell, D. J., Decline of minorities in stubborn societies, *Eur. Phys. J. B*, **57**(4), 481–486 (2007).

[59] Porter, M. A. and Gleeson, J. P., *Dynamical Systems on Networks: A Tutorial*, Springer, Switzerland (2016).

[60] R Development Core Team, R: A language and environment for statistical computing, *R Foundation for Statistical Computing*, Vienna, http://www.R-project.org (2008).

[61] Sen, P. and Chakrabarti, B. K., *Sociophysics: An Introduction*, Oxford University Press, Oxford (2013).

[62] Shang, Y., Deffuant model with general opinion distributions: First impression and critical confidence bound, *Complexity*, **19**(2), 38–49 (2013).

[63] Siegel, D. A., Social networks and collective action, *Am. J. Polit. Sci.*, **53**(1), 122–138 (2009).

[64] Sobkowicz, P., Modelling opinion formation with physics tools: Call for closer link with reality, *J. Artif. Soc. Soc. Simul.*, **12**(11), 1 (2009).

[65] Stauffer, D. and Meyer-Ortmanns, H., Simulation of consensus model of Deffuant *et al.* on a Barabási-Albert network, *Int. J. Mod. Phys. C*, **15**(2), 241–246 (2004).

[66] Sullivan, L. E., Selective exposure, *The SAGE Glossary of the Social and Behavioral Sciences*, 465 (2009).

[67] Sznajd-Weron, K. and Sznajd, J., Opinion evolution in closed community, *Int. J. Mod. Phys. C*, **11**(6), 1157–1165 (2000).

[68] Sznajd-Weron, K., Sznajd model and its applications, *Acta Phys. Pol. B*, **36**, 2537–2547 (2005).

[69] Wasserman, S. and Faust, K., *Social Network Analysis: Methods and Applications*, Cambridge University Press, Cambridge (1995).

[70] Watts, D. J. and Strogatz, S. H., Collective dynamics of 'small-world' networks, *Nature*, **393**, 440–442 (1998).

[71] Weisbuch, G., Kirman, A., and Herreiner, D., Market organization and trading relationships, *Econ. J.*, **110**(463), 411–436 (2000).

[72] Weisbuch, G., Deffuant, G., Amblard, F., and Nadal, J.-P., Meet, discuss, and segregate!, *Complexity*, **7**(3), 55–63 (2002).

[73] Weisbuch, G., Bounded confidence and social networks, *Eur. Phys. J. B*, **38**(2), 339–343 (2004).

[74] Weisbuch, G., Deffuant, G., and Amblard, F., Persuasion dynamics, *Physica A*, **353**, 555–575 (2005).

[75] West, D. B., *Introduction to Graph Theory*, Prentice Hall, New Jersey, 2nd ed. (2001).

[76] White, H, Boorman, S., and Breiger, R., Social structure from multiple networks. I Blockmodels of roles and positions, *Am. J. Sociol.*, **81**, 730–780 (1976).